

Flexible Microstrip Patch Antenna Design on Jeans Substrate Radiating at 2.45 GHz for WBAN Application

*Project report submitted to
Indian Institute of Information Technology, Nagpur,
in partial fulfillment of the requirements for the award of
the degree*

Bachelor of Technology In Electronics and Communication Engineering

by

Sakshi Pandagale (BT19ECE005)

Avish Fakirde (BT19ECE037)

Saikumar Mulkalla (BT19ECE073)

Under the guidance of

Dr. Paritosh Peshwe



*Indian Institute of Information Technology,
Nagpur 441108 (India)*

2023

Flexible Microstrip Patch Antenna Design on Jeans Substrate Radiating at 2.45 GHz for WBAN Application

*Project report submitted to
Indian Institute of Information Technology, Nagpur,
in partial fulfillment of the requirements for the award of
the degree*

Bachelor of Technology In Electronics and Communication Engineering

by

Sakshi Pandagale (BT19ECE005)

Avish Fakirde (BT19ECE037)

Saikumar Mulkalla (BT19ECE073)

Under the guidance of

Dr. Paritosh D. Peshwe



***Indian Institute of Information Technology,
Nagpur 441108 (India)***

2023

Department of Electronics and Communication Engineering

Indian Institute of Information Technology, Nagpur



Declaration

We, **Sakshi Pandagale, Avish Fakirde, Saikumar Mulkalla**, hereby declare that this project work titled "**Flexible Microstrip Patch Antenna Design on Jeans Substrate Radiating at 2.45 GHz for WBAN Application**" is carried out by us in the **Department of Electronics and Communication Engineering** of Indian Institute of Information Technology, Nagpur. The work is original and has not been submitted earlier whole or in part for the award of any degree/diploma at this or any other Institution /University.

Sr. No.	Enrollment No.	Name	Signature
1.	BT19ECE005	Sakshi Pandagale	
2.	BT19ECE037	Avish Fakirde	
3.	BT19ECE073	Saikumar Mulkalla	

Date: 19th May, 2023

Department of Electronics and Communication Engineering

Indian Institute of Information Technology, Nagpur



Declaration

We, **Sakshi Pandagale, Avish Fakirde, Saikumar Mulkalla**, Enrollment No **BT19ECE005, BT19ECE037, BT19ECE073**, understand that plagiarism is defined as any one or the combination of the following:

1. Uncredited verbatim copying of individual sentences, paragraphs or illustrations (such as graphs, diagrams, etc.) from any source, published or unpublished, including the internet.
2. Uncredited improper paraphrasing of pages or paragraphs (changing a few words or phrases, or rearranging the original sentence order).
3. Credited verbatim copying of a major portion of a paper (or thesis chapter) without clear delineation of who did or wrote what. (Source: IEEE, the institute, Dec.2004)

I have made sure that all the ideas, expressions, graphs, diagrams, etc. that are not a result of my own work, are properly credited. Long phrases or sentences that had to be used verbatim from published literature have been clearly identified using quotation marks.

I affirm that no portion of our work can be considered as plagiarism and I take full responsibility if such complaint occurs. I understand fully well the guide of the thesis may not be in a position to check for possibility of such incidences of plagiarism in this body of work.

Sr. No.	Name	Signature
1.	Sakshi Pandagale	
2.	Avish Fakirde	
3.	Saikumar Mulkalla	

Date: 19th May, 2023

Certificate

This is to certify that the project titled "**Flexible Microstrip Patch Antenna Design on Jeans Substrate Radiating at 2.45 GHz for WBAN Application**", submitted by **Sakshi Pandagale, Avish Fakirde, Saikumar Mulkalla** in partial fulfillment of the requirements for the award of the degree of **Bachelor of Technology in Department of Electronics and Communication Engineering**, IIIT Nagpur. The work is comprehensive, complete and fit for final evaluation.

Date - 19/05/2023

Dr. Paritosh Peshwe
Assistant Professor, Department of
Electronics and Communication
Engineering, IIIT Nagpur

(Industry Expert's Name)

(Academic Expert's Name)

(Industry Expert's Signature)

(Academic Expert's Signature)

(Name and Sign of HoD)
IIIT Nagpur

ACKNOWLEDGEMENT

We extend our heartfelt thanks to **Dr. Paritosh D. Peshwe**, Assistant Professor in the Department of ECE and our institute level supervisor, for his unwavering support, guidance, and encouragement throughout the project. His insights, experience, vision, and enthusiastic participation were invaluable and served as a source of inspiration for us. We are deeply grateful for his excellent mentor-ship, which has helped us achieve success in our project.

We would like to extend our sincere thanks to **Mrs. Deepika Sagne**, Junior Technical Officer in the Department of ECE, for her invaluable support and assistance in the completion of our project.

We are grateful to our departmental peers for their unwavering support and encouragement during our research endeavor. We want to express our profound appreciation to our friends, as well as to those whose names are not listed, for providing us with direct or indirect support during every circumstance, be it favorable or unfavorable.

We would like to express our sincere appreciation to **Lalitha Tanmai Vaddiparthi, Guna Sai Kiran Nekkanti**, and **Amit Yadav**, our junior fellows in the Department of ECE, for their excellent coordi-nation that greatly facilitated the completion of our project.

Lastly, we would like to express our appreciation to all individuals who have supported us in any way throughout this endeavor.

SAKSHI PANDAGALE

AVISH FAKIRDE

SAIKUMAR MULKALLA

ABSTRACT

Monitoring real-time data of human beings has become increasingly popular in various sectors such as healthcare and sports. This type of monitoring is of utmost importance in many cases, which has led to a surge of interest in Wireless Body Area Networks. These networks have emerged as a promising technology for monitoring and transmitting physiological data in a non-invasive and cost-effective manner. Typically, these networks consist of a set of wearable or implantable sensors that are attached to the human body and communicate wirelessly with a central hub or remote server. The collected data can be utilized for various applications.

Wearable antennas play a vital role in enabling WBANs to transmit physiological data reliably and accurately. However, designing such antennas requires careful attention to their physical attributes, such as size, weight, and comfort. Researchers in this field have focused on developing antennas that are both efficient and unobtrusive, using lightweight materials and a low-profile configuration to ensure that they conform to the shape of the wearer's body. These antennas must also be able to operate across a wide range of frequencies to ensure the seamless transmission of data between sensors and receivers. With the advent of modern wearable mobile devices, the demand for antennas that are smaller in size and flexible enough to fit internally has become a necessity. In the context of Wireless Body Area Networks (WBANs), designing devices that are comfortable and wearable for extended periods is a crucial consideration. This is where the importance of flexible antennas comes into play, as they have the ability to conform to the shape of the body, making them a more comfortable option even when worn for long periods.

This paper explores the design and implementation of a flexible microstrip patch antenna on a jeans substrate for Wireless Body Area Networks (WBAN) applications operating at a frequency of 2.45 GHz. The proposed design aims to provide an efficient and reliable solution. The antenna's flexibility allows it to conform to the body's shape, providing reliable communication while minimizing discomfort. Through simulation and experimental analysis, the proposed antenna's performance is evaluated and found to be suitable for WBAN applications.

Keywords: *Flexible Antenna, WBAN, Microstrip Patch Antenna, Jeans Substrate, Wearable*

TABLE OF CONTENTS

LIST OF FIGURES	v
LIST OF TABLES	viii
LIST OF ABBREVIATIONS	ix
1 INTRODUCTION	1
1.1 Motivation and Overview	1
1.2 Objectives of the Project	2
1.3 Organization of the Thesis	2
2 BACKGROUND KNOWLEDGE	3
2.1 Wireless Body Area Networks (WBAN)	3
2.2 Flexible Antennas	4
2.3 Role of Flexible Antennas in WBAN	5
2.4 Overview of Antennas	6
2.4.1 Wired Antennas	7
2.4.2 Planar Antennas	7
2.5 Importance of Patch Antenna for Flexible Antennas	7
2.6 Overview of Substrate Materials for Flexible Antennas	8
2.6.1 Dielectric constant and Loss tangent	9
2.6.2 Thickness	9
2.6.3 Flexibility	9
2.6.4 Effect of Temperature and Moisture	9
2.7 Antenna Parameters	10
2.7.1 Dielectric constant and Loss tangent	10
2.7.2 Quality Factor	10

2.7.3	Reflection Coffeicient	11
2.7.4	Resonance Frequency	11
2.7.5	Radiation Efficieny	11
2.7.6	Gain	12
2.7.7	SAR	12
3	LITERATURE REVIEW	13
3.1	Previous Research Paper	13
3.1.1	Research Paper [9]	13
3.1.2	Research Paper [10]	14
3.1.3	Research Paper [11]	14
3.1.4	Research Paper [12]	14
3.1.5	Research Paper [13]	15
3.1.6	Research Paper [14]	15
3.1.7	Research Paper [15]	15
3.1.8	Research Paper [16]	16
3.1.9	Research Paper [17]	16
3.1.10	Research Paper [18]	16
3.1.11	Research Paper [19]	17
3.1.12	Research Paper [20]	17
4	PROPOSED WORK	18
4.1	Antenna Design Flow	18
4.1.1	Antenna Design 1	18
4.1.2	Antenna Design 2	21
4.1.3	Antenna Design 3	25
5	RESULTS AND DISCUSSION	29
5.1	Performance Analysis of Proposed Antenna Designs	29
5.1.1	Antenna Design 1	30
5.1.1.1	S11 Parameter	30
5.1.1.2	Gain and radiation Efficiency	31
5.1.1.3	Specific Absorption Rate (SAR)	33
5.1.2	Antenna Design 2	34

5.1.2.1	S11 Parameter	35
5.1.2.2	Gain and radiation Efficiency	35
5.1.2.3	Specific Absorption Rate (SAR)	36
5.1.2.4	Bending Analysis	37
5.1.3	Antenna Design 3	40
5.1.3.1	S11 Parameter	41
5.1.3.2	Gain and radiation Efficiency	42
5.1.3.3	Specific Absorption Rate (SAR)	43
5.1.3.4	Bending Analysis	43
5.1.4	Comparision of the proposed antennas with previous work	46
6	CONCLUSION	48
6.1	Conclusion	48
REFERENCES		49
LIST OF PUBLICATIONS		53

LIST OF FIGURES

4.1	Evolution of patch of Antenna from iteration 0 to iteration 4	19
4.2	Evolution of ground plane of Antenna from iteration 0 to iteration 4	19
4.3	Variation of S11 of the antenna from iteration 0 to iteration 4	20
4.4	Variation of gain of the antenna from iteration 2 to iteration 4	20
4.5	Topology of final proposed antenna: (a) top view (b) bottom view	20
4.6	Evolution of patch of Antenna from iteration 0 to iteration 4	21
4.7	Evolution of ground plane of Antenna from iteration 0 to iteration 4	22
4.8	Variation of reflection coefficient (S11) of Antenna Design 1 with iterations	23
4.9	Variation of radiation pattern (gain) of antenna from iteration 0 to iteration 4	23
4.10	Topology of final proposed antenna: (a) top view, (b) bottom view and surface current distribution of the antenna at 2.45GHz (c), (d), (e)	24
4.11	Evolution of patch of Antenna from iteration 0 to iteration 3	25
4.12	Evolution of ground plane of Antenna from iteration 0 to iteration 3	26
4.13	Variation of reflection coefficient (S11) of Antenna Design with iterations	27
4.14	Variation of radiation pattern (gain) of antenna from iteration 0 to iteration 3	27
4.15	Topology of final proposed antenna: (a) top view, (b) bottom view	28
5.1	Human tissue phantom model	29
5.2	Fabricated proposed antenna (a) top view and (b) bottom view	30
5.3	Simulated S11 of the proposed antenna	31
5.4	S11 results of the proposed antenna with phantom model	31
5.5	Gain of the proposed antenna	32
5.6	Simulated radiation patterns of the proposed antenna in the (a) E-plane ($\phi = 0^\circ$) and (b) H-plane ($\phi = 90^\circ$)	32

5.7 Simulated(with phantom model) radiation patterns of the proposed antenna in the (a) E-plane ($\phi = 0^\circ$) and (b) H-plane ($\phi = 90^\circ$)	33
5.8 Measured SAR value of proposed antenna	33
5.9 Fabricated proposed antenna (a) top view and (b) bottom view	34
5.10 Testing of proposed antenna on VNA	34
5.11 Simulated, measured and with human tissue reflection coefficient (S11) of proposed antenna	35
5.12 Gain of the proposed antenna	36
5.13 Measured and simulated radiation patterns of the proposed antenna in the (a) E-plane ($\phi = 0^\circ$) and (b) H-plane ($\phi = 90^\circ$)	36
5.14 Measured SAR value of the proposed antenna	37
5.15 Structure of antenna under two bending condition with different radii, horizontal (x-axis) (a) Rx = 20 mm, (b) Rx = 40 mm, (c) Rx = 80 mm and Vertical (y-axis) (d) Ry = 20 mm, (e) Ry = 40 mm, (f) Rx = 80 mm	38
5.16 Measured and simulated S11(s) of the proposed antenna under (a) horizontal (x-axis) and (b) vertical (y-axis) bending conditions with different curvatures	38
5.17 Measured and simulated radiation patterns of the proposed antenna under horizontal (x-axis) bending condition in the (a) E-plane ($\phi = 0^\circ$) and (b) H-plane ($\phi = 90^\circ$) . .	39
5.18 Measured and simulated radiation patterns of the proposed antenna under vertical (y-axis) bending condition in the (a) E-plane ($\phi = 0^\circ$) and (b) H-plane ($\phi = 90^\circ$)	39
5.19 Fabricated proposed antenna (a) top view and (b) bottom view	40
5.20 Testing of the proposed antenna on VNA	41
5.21 Simulated, measured and with human tissue reflection coefficient (S11) of proposed antenna	41
5.22 Gain of the proposed antenna	42
5.23 Simulated radiation patterns of the proposed antenna in the (a) E-plane ($\phi = 0^\circ$) and (b) H-plane ($\phi = 90^\circ$)	42
5.24 Simulated(with phantom model) radiation patterns of the proposed antenna in the (a) E-plane ($\phi = 0^\circ$) and (b) H-plane ($\phi = 90^\circ$)	43
5.25 Measured SAR Value of the antenna	43

5.26 Structure of antenna under two bending condition with different radii, horizontal (x-axis) (a) Rx = 20 mm, (b) Rx = 40 mm, (c) Rx = 80 mm and Vertical (y-axis) (d) Ry = 20 mm, (e) Ry = 40 mm, (f) Rx = 80 mm	44
5.27 Measured and simulated S11(s) of the proposed antenna under (a) horizontal (x-axis) and (b) vertical (y-axis) bending conditions with different curvatures	45
5.28 Radiation pattern of antenna under hotizontal (x-axis) bending condition with different radii, E-plane ($\phi = 0^\circ$) and (b)(a) Rx = 20 mm, (b) Rx = 40 mm, (c) Rx = 80 mm and H-plane ($\phi = 90^\circ$)(d) Rx = 20 mm, (e) Rx = 40 mm, (f) Rx = 80 mm	45
5.29 Radiation pattern of antenna under vertical (y-axis) bending condition with different radii, E-plane ($\phi = 0^\circ$) and (b)(a) Rx = 20 mm, (b) Rx = 40 mm, (c) Rx = 80 mm and H-plane ($\phi = 90^\circ$)(d) Rx = 20 mm, (e) Rx = 40 mm, (f) Rx = 80 mm	46

List of Tables

4.1	Optimized design parameters of proposed antenna in Figure 4.5(a) and 4.5(b)	21
4.2	Optimized design parameters of proposed antenna in Figure 4.10a and 4.10b	25
4.3	Optimized design parameters of proposed antenna in Figure 4.10(a) and 4.10(b) . . .	28
5.1	Properties of human tissue phantom model	30
5.2	Comparison of antenna properties under two bending conditions with different cur- vatures	40
5.3	Comparison of antenna properties under two bending conditions with different cur- vatures	46
5.4	Comparision of proposed antennas with other wearable antennas	47

LIST OF ABBREVIATIONS

WBAN - Wireless Body Area Networks

ISM - Industrial, Scientific and Medical

DGS - Defected Ground Structure

SAR - Specific Absorption Rate

AMC - Artificial Magnetic Conductor

ICNIRP - International Commission on Non-Ionizing Radiation Protection

IEEE - Institute of Electrical and Electronics Engineers

FCC - Federal Communications Commission

MTM - Metamaterial

PIFA - Planar Inverted-F Antenna

Chapter 1

INTRODUCTION

This chapter provides a brief overview, motivation, and importance of research on flexible antennas for WBAN.

1.1 Motivation and Overview

Motivation for our thesis come from the increasing demand for WBAN applications, which have become popular in recent years due to their ability to provide real-time health monitoring and diagnosis, as well as other medical applications [1]. However, one of the key challenges in designing WBAN antennas is the need for a flexible and comfortable substrate that can conform to the human body, without causing discomfort or irritation. However, to ensure accurate and reliable monitoring, WBAN antennas must meet certain requirements. They must be small, lightweight, and conformable to the human body, while also being able to operate in a confined space and transmit and receive signals with high efficiency. These requirements pose significant challenges for antenna design.

Microstrip patch antennas are popular for WBANs because they are lightweight, low profile, and easy to integrate with electronic circuits. They consist of a thin metal patch on a dielectric substrate and have a wide range of operating frequencies, making them suitable for various applications [2]. Jeans substrate is a low-cost and widely available material that is flexible, lightweight, and bio-compatible. It is preferred over traditional substrates like polyester or polyimide because it offers greater conformability to the human body, resulting in increased comfort for the wearer.

In this project, we have designed a compact, low-profile, and flexible antenna on a jeans substrate that resonates at the ISM frequency band of 2.45 GHz. We have obtained its parameters to ensure that it is suitable for on-body applications.

1.2 Objectives of the Project

- To Design a compact and flexible microstrip patch antenna.
- Achieve impedance matching of the antenna at 2.45 GHz.
- Ensure reliable radiation efficiency of the antenna suitable for on-body applications.
- Minimize the Specific Absorption Rate (SAR) of the proposed antenna.
- Perform bending analysis to test the flexibility of the antenna.

1.3 Organization of the Thesis

The report presents the project work in the form of 6 chapters, each of which is briefly described below and structured accordingly:

- **Chapter 1** provides a brief overview, motivation, and importance of research on flexible antennas for WBAN.
- **Chapter 2** deals with providing an explanation of important background topics that are necessary for understanding the thesis, such as WBAN, flexible antennas, and general antenna parameters.
- **Chapter 3** gives a better understanding and highlights remarkable milestones achieved by previous researchers in this domain, thus paving the way for further improvements.
- **Chapter 4** provides a comprehensive insight into the proposed antennas, outlining the detailed design process that has been undertaken to ensure superior performance.
- **Chapter 5** focuses on presenting the results and evaluating the performance of the proposed antenna designs. It also conducts a comparative analysis of the proposed antennas with existing wearable antennas.
- **Chapter 6** provides a concluding summary of the entire project.

Chapter 2

BACKGROUND KNOWLEDGE

This Chapter deals with providing an explanation of important background topics that are necessary for understanding the thesis, such as WBAN, flexible antennas, and general antenna parameters.

2.1 Wireless Body Area Networks (WBAN)

Wireless Body Area Network (WBAN) refers to a wireless network of wearable devices that can be attached to or implanted into the human body, allowing for real-time monitoring and data collection. This technology holds significant promise and has diverse potential applications in areas such as healthcare, sports and fitness, and military and emergency response.

A typical WBAN comprises three primary components sensors, communication devices, and a data processing unit. The sensors collect physiological and environmental data such as heart rate, blood pressure, and temperature. The communication devices transmit this data wirelessly from the sensors to the data processing unit, which is responsible for analyzing and processing the data. Additionally, the data processing unit can communicate with external devices, such as smartphones or medical equipment, to provide feedback or alerts.

WBAN can be used for continuous health monitoring, rehabilitation and physical therapy, and remote patient monitoring in healthcare. For example, WBAN can monitor patients with chronic conditions, such as diabetes or heart disease, to provide real-time feedback and alerts to healthcare providers. WBAN can also aid in rehabilitation and physical therapy, where wearable sensors can track a patient's progress and provide feedback on their exercises. Remote patient monitoring is another application of WBAN, which enables patients to be monitored from their homes, reducing the need for hospital visits.

In sports and fitness, WBAN can be used for performance tracking and injury prevention. Wearable sensors can track a player's movements, heart rate, and other physiological data, providing insights into their performance and potential injury risks. Coaches and trainers can use this data to adjust training routines and prevent injuries.

In military and emergency response, WBAN can be used for tracking soldiers and first responders in hazardous environments. Wearable sensors can track a soldier's location, health status, and other important data, providing commanders with real-time feedback on their troops status. First responders can also benefit from WBAN, where wearable sensors can track their location and vital signs, providing situational awareness to other responders.

However, WBAN faces several challenges that need to be addressed, including security and privacy concerns, power consumption, interference and reliability issues, and cost. As these devices are attached to or implanted into the human body, they can potentially be hacked, compromising the privacy and security of the wearer. Power consumption is another issue as the devices rely on batteries with limited capacity. Interference and reliability issues can also affect the performance of WBAN, especially in crowded environments. Lastly, the cost of manufacturing and maintaining these devices can be significant.

2.2 Flexible Antennas

Flexible antennas are antennas that are designed to be flexible and conformable to the human body. They can be made from a variety of materials, such as metal foils, conductive textiles, and conductive polymers. Flexible antennas can be integrated into wearable devices, such as smartwatches, fitness trackers, and medical sensors, enabling wireless communication between the devices and external sources.

Flexible antennas are a critical component of flexible electronics, a rapidly growing field with a broad range of potential applications. Flexible antennas offer several advantages over traditional rigid antennas, including the ability to conform to complex shapes and the potential for integration with other flexible components.

These antennas are already finding applications in numerous fields, including healthcare, consumer electronics, and environmental sensing. For instance, wearable devices with flexible antennas can monitor a patient's vital signs or track physical activity without restricting their movements. Additionally, flexible antennas can be integrated into clothing or accessories to facilitate wireless communication or data transfer, creating opportunities for smart textiles.

They are also essential in the development of flexible displays, which are poised to revolutionize consumer electronics. These antennas can be integrated into displays to provide wireless connectivity, enabling the creation of devices with foldable or rollable screens that can connect to the internet or other devices. Recent advances in the design of flexible antennas have focused on improving their performance, reliability, and ease of manufacturing. One such advance is the use of new materials, such as liquid metal and graphene, which offer higher conductivity and flexibility than traditional materials. Another advance is the use of new fabrication techniques, such as 3D printing and ink-jet printing, which allow for the rapid prototyping and mass production of flexible antennas.

Flexible antennas face several design challenges, including bandwidth, efficiency, and impedance matching. Bandwidth is a measure of the range of frequencies over which an antenna can operate effectively. For wearable devices, it is essential to have a wide bandwidth to ensure reliable communication over a range of frequencies. Efficiency is a measure of how much power the antenna can radiate compared to the power it receives. In wearable devices, where battery life is a critical concern, it is essential to have an efficient antenna that can minimize power consumption. Impedance matching is a measure of how well the antenna is matched to the input impedance of the wireless transceiver. Poor impedance matching can result in signal loss and reduced communication range.

2.3 Role of Flexible Antennas in WBAN

Wireless Body Area Networks (WBANs) have emerged as a promising technology for healthcare and sports applications. WBANs consist of miniature wireless devices, sensors, and antennas that are placed on or inside the human body to monitor various physiological parameters, such as heart rate, temperature, blood pressure, and blood glucose levels. Flexible antennas play a critical role in enabling WBANs to operate effectively and efficiently.

Flexible antennas are particularly well-suited for WBANs because they can be conformally integrated with the human body, enabling accurate and reliable sensing of physiological parameters. In addition, flexible antennas can provide better signal-to-noise ratio (SNR) and reduce interference compared to rigid antennas, leading to improved data transmission and reception. The flexibility of the antennas also reduces the risk of discomfort or injury to the patient, making WBANs more user-friendly.

These antennas can be made from a range of materials, including polymers, metal foils, and conductive fabrics, which allow them to be easily bent or twisted without breaking.

They are also lightweight and can be integrated into wearable devices with minimal impact on their size and weight, making them ideal for use in WBANs. The use of flexible antennas in WBANs also enables the development of more comfortable and discrete wearable devices, which are critical for long-term use and patient compliance.

Moreover, the performance of the antenna is crucial to the effectiveness of the WBAN, and flexible antennas have been shown to offer excellent performance in a variety of scenarios. They can be designed to operate in a wide range of frequency bands and have high radiation efficiency, which allows for the transmission and reception of wireless signals with minimal loss or interference.

Furthermore, flexible antennas are also well suited for use in WBANs due to their ability to conform to different shapes and sizes. This flexibility makes it possible to design antennas that can be integrated into various wearable devices, including clothing, jewelry, and even implants, without compromising their functionality.

In addition to their physical properties, flexible antennas can also be designed to support various wireless communication protocols, such as Bluetooth, Wi-Fi, and Zigbee. These protocols enable the wireless transmission of data and enable the real-time monitoring and analysis of vital physiological data.

2.4 Overview of Antennas

There are many types of antennas but can be categorized majorly into two categories.

- Wired Antennas
- Planar Antennas

2.4.1 Wired Antennas

A wire antenna is a type of antenna that is made up of a single wire or a set of wires, and it is used for transmitting or receiving electromagnetic waves. These antennas are commonly used in communication systems due to their simple design and low cost. Wire antennas can be designed in various shapes and sizes, such as dipole, monopole, and loop antennas. Wire antennas have a wide range of applications in various communication systems. For example, dipole antennas are commonly used in radio broadcasting and amateur radio applications, while monopole antennas are often used in mobile communication devices, such as cell phones and walkie-talkies. Loop antennas are used in applications that require high sensitivity, such as magnetic resonance imaging (MRI) and radio astronomy.

2.4.2 Planar Antennas

A planar antenna is a two-dimensional or flat antenna. It is constructed of conductive material that has been printed or etched into a thin, flat substrate, such as a printed circuit board. It has got significant benefits over conventional three-dimensional antennas and can = be created in a variety of sizes and forms, such as patch, slot, or microstrip antennas. Planar antennas are excellent for applications where space is limited, such as in mobile phones, Wi-Fi routers, and satellite communication systems. These antennas are small, low-profile, and simple to connect with other electronic components. They can be produced using common printed circuit board fabrication methods, which lowers the price and complexity of manufacturing.

2.5 Importance of Patch Antenna for Flexible Antennas

Due to its many benefits, including its low profile, lightweight, and simplicity of production, patch antennas are a popular option for usage in flexible antennas. A metal patch that is typically half a wavelength long makes up a microstrip antenna. In order for the antenna to function as a resonator, the length is kept constant. The ground plane is attached to the metal patch, and the gap between is filled with a dielectric material. Antennas must typically be tiny, light, and flexible in order to be integrated into clothes. Because they are usually very thin, patch antennas work well in flexible antennas

[3]. This is so that flexible antennas may bend and flex without breaking or losing their functioning, something low-profile patch antennas are less likely to do. Patch antennas may be made to function at various frequencies and polarisations(linear and circular) by adding slots and adjusting the length of the patch, making them adaptable enough to be used in a range of wearable applications, including communication devices, fitness trackers, and medical monitoring. The metallic ground plane that the patch antenna is linked with may considerably minimise the amount of energy absorbed by the body when placed between the body and the radiating parts, which is one of the key benefits of using it as a wearable application. However, conventional antennas like monopoles and dipoles lack a ground plane, and as a result, their radiation patterns are harmful to the body. Hence, a patch antenna is preferred.

Patch antennas may be made to have a broad bandwidth, allowing them to function over a variety of frequencies. This is crucial for flexible antennas because they must be able to function in various settings and circumstances even after becoming distorted. A microstrip patch antenna can be fed using a variety of techniques, including a microstrip line feed, a coaxial probe feed, a proximity-coupled feed, etc. Microstrip Line Feed has been used to feed the antenna as in this kind of feed, the patch antenna and microstrip feed line are directly connected. The microstrip line feeding system and patch antenna are simple to construct and match. Using common printed circuit board (PCB) technology, patch antennas are rather simple to manufacture. This implies that they may be made inexpensively and in great quantities, which is crucial for flexible antennas that may need to be changed or repaired often [4]. A wearable antenna must be compact, directional, flexible and have wide bandwidth, so it is simple to satisfy all of these requirements with a patch antenna.

2.6 Overview of Substrate Materials for Flexible Antennas

A dielectric material is utilised between the metal patch and the ground plane. When evaluating antenna performance, the dielectric constant is crucial. The term "substrate" also applies to the dielectric substance. A variety of dielectric materials are used in the construction of wearable antennas. These materials were selected with care to offer a suitable level of mechanical deformations with little impact from various weather conditions and appropriate EM radiation protection. Wearable antennas, which may be used in WBAN, are created to function while being worn. Because these antennas work so close to the human body, appropriate materials must be used in their design [5]. Below is a

discussion of the substrate's characteristics that have an impact on the performance of the wearable flexible textile antenna and were taken into consideration while selecting denim jeans as a substrate for designing a patch antenna.

2.6.1 Dielectric constant and Loss tangent

As the value of $\tan(\delta)$ grows, the patch antenna's efficiency and gain drop, however, bandwidth improves as the substrate's dielectric losses rise [6]. The feed location must be adjusted away from the centre of the patch antenna in order to employ substrate with high losses since the input resonance resistance decreases as the value of tan increases. Resonance frequency falls down as relative permittivity (ϵ_r) increases. The overall quality factor increases and the fringing fields decline as the bandwidth lowers with an increase in the dielectric constant [7].

2.6.2 Thickness

Resonance frequencies decrease as substrate thickness(h) increases, which contributes to an increase in effective patch size. The overall quality factor increases and the fringing fields decline as the bandwidth lowers with a decrease in the substrate thickness. The rise in aperture area and patch size is what causes the efficiency, gain, and directivity to increase as substrate thickness increases.

2.6.3 Flexibility

To ensure comfort and suitability for body-worn antennas, traditional designs often employ materials that may be unpleasant. However, for wearable antennas to be comfortable for users, it is crucial to utilize flexible substrates. As the antenna is shaped to conform to the human body, the substrate's thickness will naturally undergo slight changes due to elongation, thereby affecting the performance characteristics of the patch antenna.

2.6.4 Effect of Temperature and Moisture

In the literature study, it was found that there is a linear, frequency-independent connection between the change in temperature and the change in dielectric constant. The calculated value was $\Delta\epsilon_r = 1.67 \times 10^{-3}$ per degree Celsius [8]. By linearly extrapolating the relationship, it becomes possible to reach any temperature value. When textiles absorb water, their electromagnetic properties are modified, resulting in an increase in both the dielectric constant and loss. Moreover, the cloth

substrate used in body-worn antennas can accumulate moisture from the skin, subsequently affecting the antenna's functionality. The close proximity of the body-worn antenna to the body leads to an increase in the effective permittivity, thereby reducing the Q factor of the antenna.

2.7 Antenna Parameters

2.7.1 Dielectric constant and Loss tangent

The quantity of electric potential energy, in the form of induced polarisation, that is stored in a certain volume of material under the influence of an electric field is quantified by the dielectric constant. It is quantified as the ratio of the material's dielectric permittivity to that of dry air or a vacuum.

$$k = \frac{C}{C_0}$$

where, C is permittivity of the substance, C_0 is permittivity of a vacuum.

Loss tangent, also known as dielectric loss tangent, is a measure of how much energy is lost as heat when an alternating current (AC) electric field is applied to a dielectric material. It is the ratio of the imaginary part of the dielectric constant (representing energy loss) to its real part (representing energy storage) for a material under an AC electric field.

$$k = \frac{\epsilon''}{\epsilon'}$$

where, ϵ' is the real part of the dielectric constant (i.e., the permittivity) of the material, and ϵ'' is the imaginary part of the dielectric constant (i.e., the loss factor) of the material.

2.7.2 Quality Factor

The Q factor is defined as the ratio of the resonant frequency to the bandwidth of the antenna.

$$Q = \frac{f_c}{\Delta f}$$

where, f_c is resonance frequency of antenna, Δf is bandwidth of antenna.

A higher Q factor indicates that the antenna has a narrower bandwidth and is more selective in transmitting or receiving signals at the resonant frequency.

2.7.3 Reflection Coffeicient

It quantifies how much of an electromagnetic wave is reflected by an impedance discontinuity in the transmission medium i.e. between transmission line and patch antenna. The reflection coefficient is equal to the ratio of the amplitude of the reflected wave to the incident wave.

$$\Gamma = \frac{Z_L - Z_0}{Z_L + Z_0}$$

where, Z_L is Load impedance of patch, Z_0 is Characteristic impedance of the transmission line.

2.7.4 Resonance Frequency

The resonance frequency of an antenna is the frequency at which the antenna exhibits maximum efficiency and receives or radiates the most power. At resonance, the antenna's input impedance becomes purely resistive, and its reactance becomes zero. This means that the antenna is well-matched to the transmission line or feed network, and there is no reflected power. The resonance frequency is the frequency at which an antenna is designed to operate.

$$f_r = \frac{c}{2(L + H)\sqrt{\epsilon_r}}$$

The resonant frequency of antenna is determined by both the length and the width of the antenna.

2.7.5 Radiation Efficieny

The radiation efficiency of an antenna is a crucial parameter that quantifies the antenna's ability to convert electrical power into radiated electromagnetic energy. It represents the ratio of the power radiated by the antenna to the total input power supplied to the antenna. A high radiation efficiency indicates a more efficient antenna, minimizing power losses within the antenna structure. Factors such as antenna design, materials, and environmental conditions influence the radiation efficiency. Understanding and optimizing the radiation efficiency of antennas is essential for maximizing their

performance and ensuring effective transmission and reception of electromagnetic signals.

$$\eta = \frac{P_{rad}}{P_i}$$

where, P_{rad} is the power radiated by the antenna and P_i is the total input power supplied to the antenna.

2.7.6 Gain

The term Antenna Gain describes how much power is transmitted in the direction of peak radiation to that of an isotropic source. Antenna Gain (G) can be related to directivity (D) and antenna efficiency by,

$$G = e \times D$$

where, e is the antenna efficiency, D is the directivity of antenna.

Gain of antenna is also given by the formula

$$G_{dB} = 10 \log_{10} \left(\frac{4\pi\eta A}{\lambda^2} \right)$$

where, η is the efficiency, A is the physical aperture area and λ is the wavelength of the signal.

2.7.7 SAR

The Specific Absorption Rate (SAR) is a measurement of the amount of electromagnetic energy absorbed by the human body when exposed to radio frequency electromagnetic fields (RF-EMF). It is typically quantified in watts per kilogram (W/kg), using the formula,

$$SAR = \frac{\sigma E^2}{\rho}$$

where σ represents the electrical conductivity of the tissue in Siemens per meter (S/m), E is the electric field strength in volts per meter (V/m), and ρ denotes the tissue density in kilograms per cubic meter (kg/m^3).

Chapter 3

LITERATURE REVIEW

This Chapter gives a better understanding and highlights remarkable milestones achieved by previous researchers in this domain, thus paving the way for further improvements.

3.1 Previous Research Paper

3.1.1 Research Paper [9]

Essence

The high gain dual resonant textile microstrip patch antenna with extended ground plane suitable to be employed for satellite Ku band uplink and downlink communication applications has been proposed in this paper. The proposed textile antenna has been fabricated over the wearable textile material - Denim as a substrate having dielectric constant $\epsilon_r = 1.6$. The radiating patch and the ground plane are designed using copper of thickness 0.05 mm and conductivity of 5.58×10^6 Siemens/m. The designed textile antenna is dual resonant at 12.64 GHz and 13.515 GHz with operating bandwidth of 1.57 GHz (12.4 GHz - 13.97 GHz) and minimal return loss of -71.86 dB and -26.28 dB, respectively. The antenna has high gain of 8.25 dB at 12.64GHz and 6.14dB at 13.515GHz and directivity of 7.97dBi at 12.64GHz and 5.8dBi at 13.515GHz. The proposed antenna has been designed and simulated using CST Microwave Studio 2014. The proposed textile antenna can be suitably employed for Ku-band applications in vehicle mounted earth stations (12.5GHz - 12.75GHz), space research and VSAT applications (12.75GHz - 13.5GHz). The simulated antenna has been practically fabricated and tested using E5071C Network Analyzer and anechoic chamber. It has been concluded that the practical results closely match with the simulated antenna results.

3.1.2 Research Paper [10]

Essence

In this paper, a compact square microstrip antenna with compact size is designed to cover 2.45GHz ISM band. The antenna geometry incorporates a circular slot. Circular polarization is achieved by using truncating corner technique. This antenna is excited by co-axial feed. It is printed on flexible substrate (jeans cloth material). Meta-material structure is also used to improve the gain of the antenna[36]. The dielectric constant for the jeans substrate is 1.7 and thickness is 1.5mm. Dimensions of the antenna are 65 mm x 65 mm x 1.5 mm, and the patch dimensions are 46 mm x 46 mm. The results of the compact, flexible microstrip antenna in term of return loss, axial ratio, radiation pattern and gain analyzed and compared with and without metamaterial antenna. The introduced of metamaterial is used to enhance the gain of the antenna. A good simulated operating frequency bandwidth (2.34 GHz – 2.50 GHz) with an axial ratio (AR) bandwidth (2.34 GHz – 2.5 GHz) and gain of 3.870 dB is presented.

3.1.3 Research Paper [11]

Essence

This paper presents the design and analysis of a compact and flexible textile antenna for wireless body-area network systems. The presented antenna operates at a frequency range of 2.2 GHz to 17 GHz and covers the UWB frequency band. The antenna is designed from a jeans textile substrate with attractive features such as flexible and low dielectric properties. Copper tape was used for the radiator patch and ground plane of the antenna. The dimensions of antenna are 45 mm x 60 mm x 1 mm. In this study, the UWB antenna successfully evaluated the return loss (S11) and radiation pattern parameters under the planar condition and various bending conditions. It has been observed that the simulation result values of the antenna are suitable for UWB WBAN applications under planar condition and different bend conditions.

3.1.4 Research Paper [12]

Essence

This paper presents a wearable planar printed meandering monopole textile antenna design having operating frequency of 2.4 – 2.45 GHz on 3 flexible substrate materials: Jeans, Leather and Cordura®. The printed elements have been designed by using a mender line technique to reduce the size of the

antenna significantly than the proposed antennas of past literature. The simulated maximum SAR was 1.14873 W/kg for 1g of tissue which satisfies the IEEE and ICNIRP standards of SAR of 1g of tissue which is 1.6 W/kg with a gain of 2.061 for jeans substrate. The compact design and miniature size of the antenna is suitable for easy integration in smart clothing for tracking, healthcare, security and other ISM applications.

3.1.5 Research Paper [13]

Essence

The creation of a brand-new, low-profile, ultra-wideband textile antenna for use in wearable medical imaging systems. The suggested antenna is based on a monopole construction. An optimized compact antenna((70 mm x 50mm) having ultra-wide bandwidth(109% between 1.198 and 4.055 GHz) is obtained by introducing two triangles and a few parallel slots at the bottom corners and top edge of the radiation patch, respectively. The antenna has a gain of 2.9 dBi. The antenna can maintain its function even when bent, working near tissue-imitating phantoms, or being used in a situation where there has been a bone fracture, demonstrating that it can react to various sizes of bone cracks.

3.1.6 Research Paper [14]

Essence

This research investigates the impact of folding on two types of antenna designs, exhibiting, respectively, folding-dependent and folding-independent electromagnetic (EM) performance. The resonance frequency of an accordion-based foldable monopole was first demonstrated to rise by 44.5% when its vertical length was cut in half. The resonance frequency of a rectangular foldable patch was then demonstrated to only slightly increase by 3.5% when its length or breadth was cut in half. In contrast to antennas that keep their EM performance despite changes in their constituent geometry, these designs provide special potential for antennas that reconfigure their EM performance. Thus, foldable antennas that may change their operating frequency in accordance with application requirements are introduced.

3.1.7 Research Paper [15]

Essence

The proposed wearable textile antenna works at 1.575 GHz and 2.45 GHz, respectively, for WBAN

and WLAN applications (S_{11} less than -15). It has dual-band characteristics. To lessen backward radiation (SAR is below 0.12 W/kg) and increase antenna gain with realised gains of 1.94 dBi and 1.98 dBic, respectively, an antenna backing based on an artificial magnetic conductor (AMC) plane operating at 2.45 GHz band is presented. The size of the antenna is $85.50 \times 85.50 \times 5.62 \text{ mm}^3$.

3.1.8 Research Paper [16]

Essence

This journal article aims for an antenna with a compact size ($55 \times 40 \times 0.125 \text{ mm}^3$), low profile, and straightforward setup. The antenna has DGS, which helps to boost its gain (2.6 dBi) and band width (1.77 - 6.95 GHz) without compromising its compactness. The antenna resonates at 2.6 GHz and has an S_{11} value of less than -30. The performance of the antenna remains mostly steady even when bent at different angles.

3.1.9 Research Paper [17]

Essence

The authors have presented a concise planar dipole antenna that operates on fully flexible nitrile butadiene rubber polymer composite and resonates at 2.46 GHz with a remarkable reflection coefficient of -20 dB. The antenna demonstrates a maximum gain of -0.96 dBi in free space, and its overall dimensions are $58 \text{ mm} \times 48 \text{ mm} \times 3.5 \text{ mm}$. However, there is scope for further improvement in the dimensions and gain of the antenna. Additionally, it is essential to note that the SAR value measured on a human tissue model with a 2mm offset is 0.204 W/kg for 1 g of tissue, which could be further reduced. The authors have not depicted the antenna's performance under bending, which should be addressed to confirm the antenna's flexibility.

3.1.10 Research Paper [18]

Essence

The journal showcases a compact and highly flexible slot antenna on a polyimide substrate that resonates at 2.45 GHz, exhibiting a remarkable reflection coefficient below -20 dB. To confirm the antenna's flexibility, the authors also conducted a bending analysis. Despite the antenna's small overall size, it initially exhibited a low gain of -12 dB without a metamaterial (MTM) array. However, after integrating the antenna with a 2x2 MTM array of $80 \text{ mm} \times 80 \text{ mm}$, a 3 dB gain enhancement was ob-

served, resulting in a final gain of -9 dB. This outcome provides an avenue for further improvement in the antenna's gain. It is essential to note that the SAR value of the antenna is outside the limits set by the FCC and IEEE, highlighting the need for improvement in this aspect as well.

3.1.11 Research Paper [19]

Essence

The article presents a compact and low-profile triangular patch antenna designed with a Koch fractal pattern. The antenna operates at 2.45 GHz on a Roger RT/duroid substrate, exhibiting a remarkable reflection coefficient below -30 dB. With a peak gain of 2.06 and a radiation efficiency of 75%, this antenna is both compact and efficient. The impedance bandwidth of the antenna is 7.75%, but there is still room for improvement in both gain and impedance bandwidth. The substrate utilized is semi-flexible, and further reduction in the antenna's SAR is possible.

3.1.12 Research Paper [20]

Essence

This paper introduces a PIFA antenna that is designed on a jeans substrate, resonating at 2.45 GHz, with a reflection coefficient below -14 dB. In free space, the antenna achieved a gain of 2.69 dBi with an area of $50 \times 16 \text{ mm}^2$. Despite its impressive performance, there is still potential for improvement in the antenna's gain. Moreover, while the SAR value of the antenna is currently within the limits established by the FCC and IEEE, there is still room for reduction. Finally, it may be possible to further minimize the antenna's dimensions.

Chapter 4

PROPOSED WORK

This chapter provides a comprehensive insight into the proposed antennas, outlining the detailed design process that has been undertaken to ensure superior performance.

In this thesis, we propose three different microstrip patch antenna structures, each of which underwent several iterations before achieving good performance suitable for WBAN. The design flow of each antenna is elaborated below.

In [21], various substrate materials were discussed for antenna fabrication, and it was determined that a Jeans material (with $\epsilon_r = 1.67$ and loss tangent $\tan\delta = 0.025$) having a thickness of 0.5 mm was used as a substrate to achieve the desired flexibility for the antenna. A 50Ω transmission line backed with a defected ground structure (DGS) was employed to excite the radiating element. Initially, the dimensions of the patch and feed were calculated using standard equations for microstrip patch antennas found in [22]. The final design of the antenna is a modified form of the conventional patch antenna. The ground plane was modified, and slots were etched to make the antenna resonant at the desired frequency and to obtain significant gain.

4.1 Antenna Design Flow

4.1.1 Antenna Design 1

The first iteration for this antenna started with a basic design of a patch antenna with full ground and no slots in the patch or ground, fed via a microstrip line as seen in Figure 4.1a and 4.2a. The antenna was resonating at 3.69 GHz gain was -0.5593 dBi and S11 as 0.106 dB.

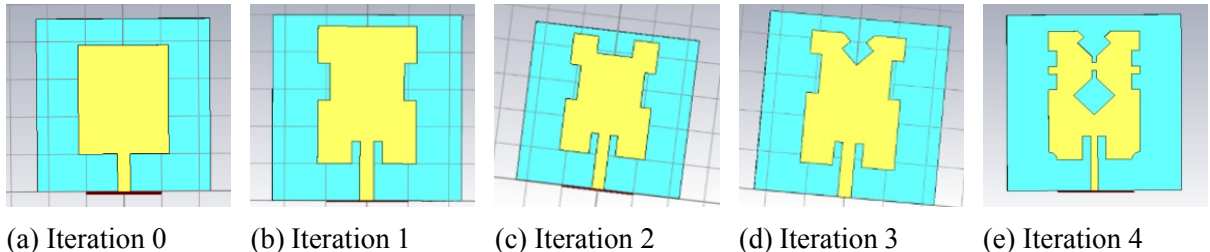


Figure 4.1: Evolution of patch of Antenna from iteration 0 to iteration 4

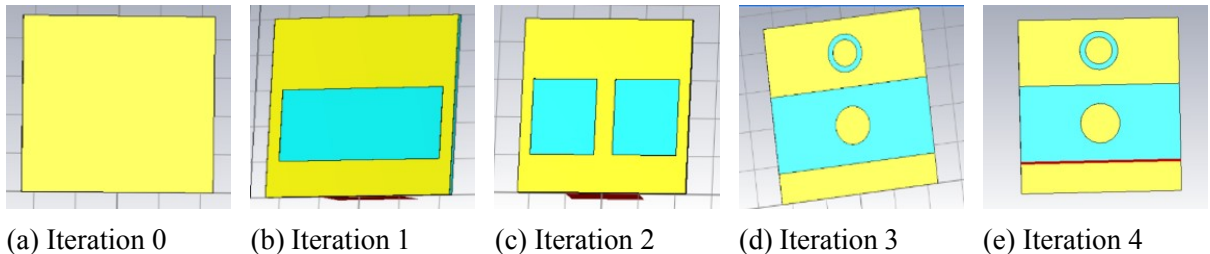


Figure 4.2: Evolution of ground plane of Antenna from iteration 0 to iteration 4

Iteration 0 showed a resonance frequency of 3.69 GHz and an S11 value greater than -10 dB. However, these were not our desired values. Slots were made in Iteration 0 to obtain Iteration 1 as shown in figures 4.1b and 4.2b, which gave us a resonance frequency of 2.2245 GHz, an S11 of -5.4597 dB, and a gain of -2.056 dBi. Since we needed a higher and positive gain, more changes were made to the ground and plate. Iteration 2 shown in figures 4.1c and 4.2c gave us a resonance frequency of 2.7075 GHz, an S11 of -31.4597 dB, and a gain of +2.056 dBi. Iteration 3 shown in figures 4.1d and 4.2d gave us a 2.7075 GHz resonance frequency and S11 as -31.717 dB. We now have desirable values for gain and S11, however, We still need to get our resonance frequency close to 2.45 GHz. In iteration 3, the slot shape in the ground and patch was changed, which gave us a resonance frequency of 2.45 GHz and -28.38687 dB as S11 and a gain of 1.918. The final iteration shown in figures 4.1e and 4.2e gave us a better S11 of -29.23266, resonance frequency, 2.45 GHz and gain as 1.83 dBi. Figure 4.3 and 4.4 illustrate the change in S11 and radiation pattern (gain) for all the iterations.

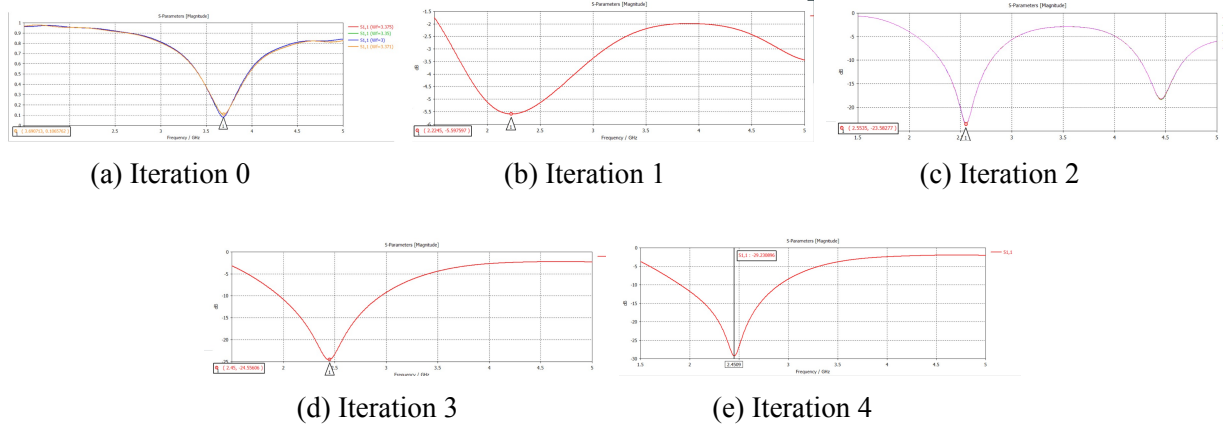


Figure 4.3: Variation of S11 of the antenna from iteration 0 to iteration 4

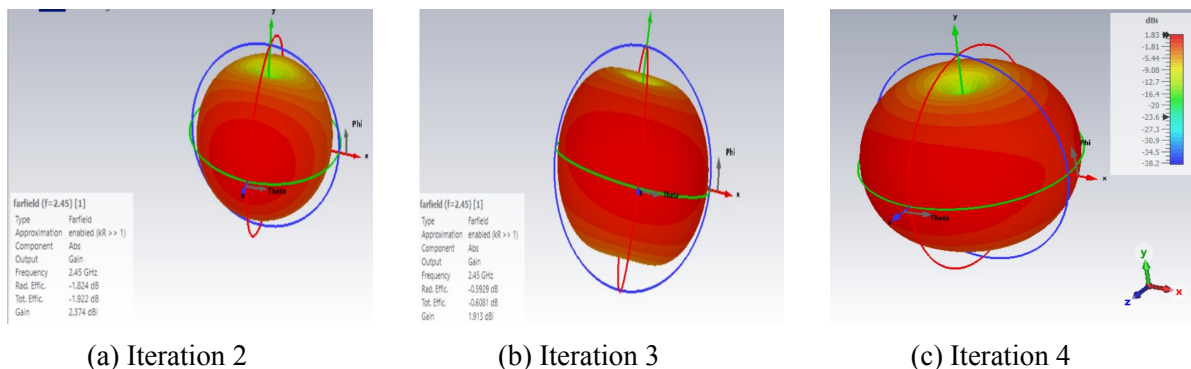


Figure 4.4: Variation of gain of the antenna from iteration 2 to iteration 4

Figures 4.5a and 4.5b exhibit the superior top and bottom views of the proposed antenna, respectively. After its ultimate iteration, the optimized parameters of the antenna are enumerated in Table 4.1.

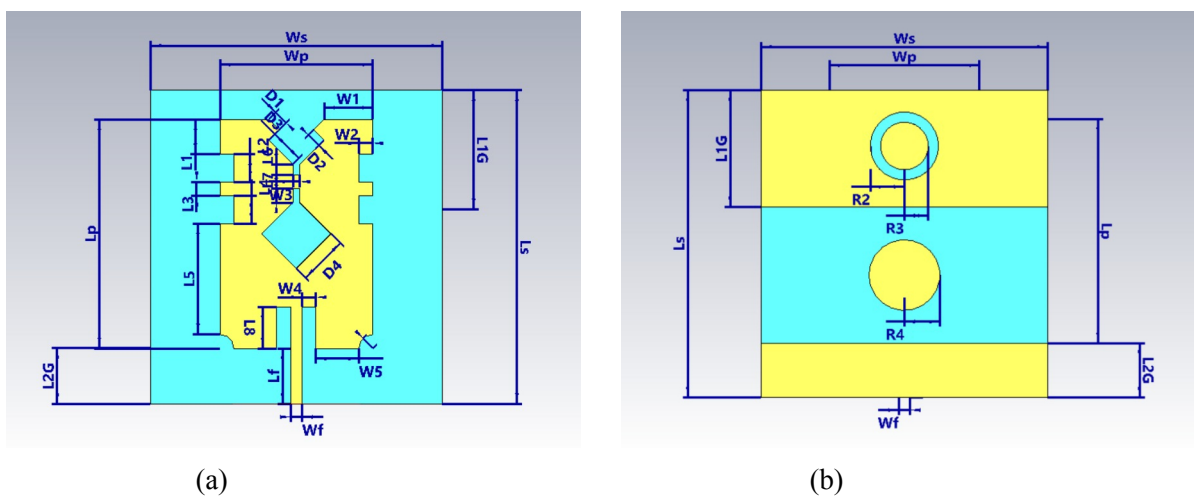


Figure 4.5: Topology of final proposed antenna: (a) top view (b) bottom view

Table 4.1
Optimized design parameters of proposed antenna in Figure 4.5(a) and 4.5(b)

Dimensions (unit: mm)						
Ws = 42	Ls = 45.2	Wp = 22	Lp = 33	Wf = 1.64	Lf = 8	L1 = 5
L2 = 4	L3 = 2	L4 = 4	L5 = 16	L6 = 1.5	L7 = 2	L8 = 6
W1 = 7	W2 = 2	W3 = 1	W4 = 2	W5 = 8.18	L1G = 17.2	L2G = 8
R1 = 2	R2 = 5	R3 = 3.5	R4 = 5.2	D1 = 2.12	D2 = 2.12	D3 = 4.95
D4 = 7.07	$t = 0.05$			$h = 0.5$		

The performance of antenna design 1 was discussed in section 5.1.1 of chapter 5. Although the antenna meets the necessary performance requirements for the WBAN, there is room for improvement in terms of size, gain, and radiation efficiency. This potential for enhancement has prompted us to propose an alternative antenna design.

4.1.2 Antenna Design 2

The design process of this antenna began with the conventional patch antenna with a full ground in iteration 0 as shown in figure 4.6a and 4.7a. This antenna had a resonance at around 3.732 GHz and a gain of 0.377 dBi. To shift the resonance to the desired frequency, the antenna was modified in iteration 1 as shown in figure 4.6b and 4.7b, by etching a circular slot and two rectangular slots on

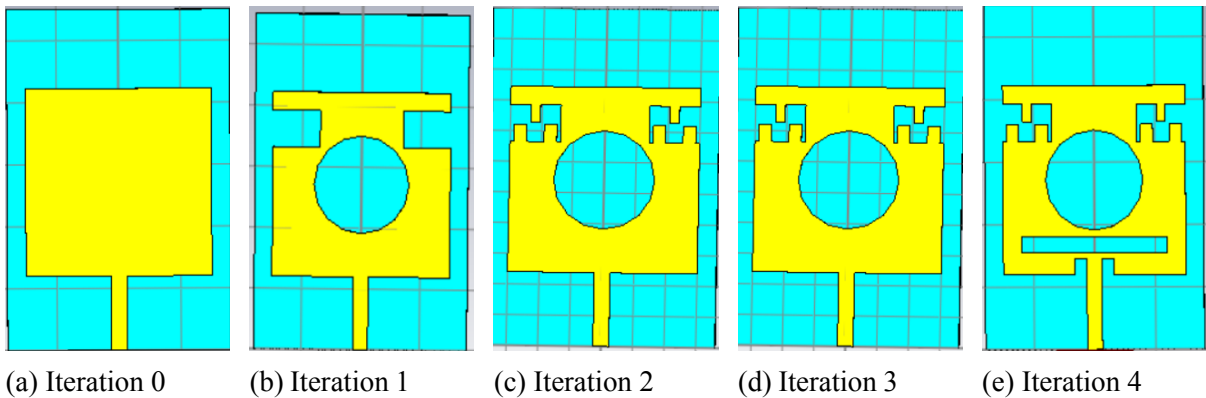


Figure 4.6: Evolution of patch of Antenna from iteration 0 to iteration 4

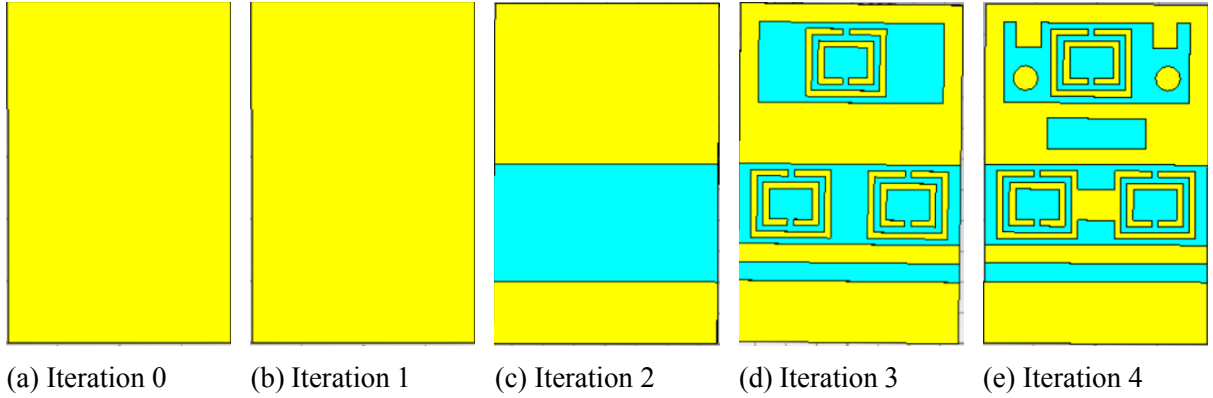


Figure 4.7: Evolution of ground plane of Antenna from iteration 0 to iteration 4

the patch to divert the current path, thereby increasing the electrical length of the antenna and shifting the resonance to the left. At this iteration, the antenna resonated at 2.48 GHz, but the S11 value was not below -10 dB, and the gain was also negative. To make the S11 value below -10 dB, impedance matching was required and the DGS structure could significantly improve the gain of the antenna [23]. Therefore, the antenna in iteration 1 was modified in iteration 2 as shown in figure 4.6c and 4.7c by placing extra copper in the top rectangular slots so that the effective gap decreased, and a rectangular slot was cut down in the ground. These slots increase the capacitance of the antenna, which matched the impedance and the DGS improved the gain. At this iteration, the antenna resonated at 2.04 GHz, the S11 was below -10 dB, and it had a better gain than the previous iteration. To shift the resonance to 2.45 GHz, the antenna in iteration 2 was modified in iteration 3 as shown in figure 4.6d and 4.7d by placing split-ring resonators on the ground plane. Split-ring resonators can act as an artificial magnetic conductor (AMC) when placed on a grounded dielectric substrate. The addition of extra copper reduced the capacitance, shifting the resonance to the right while maintaining or improving the gain. In this iteration, the antenna resonated at 2.66 GHz, the S11 was below -10 dB, and it had a

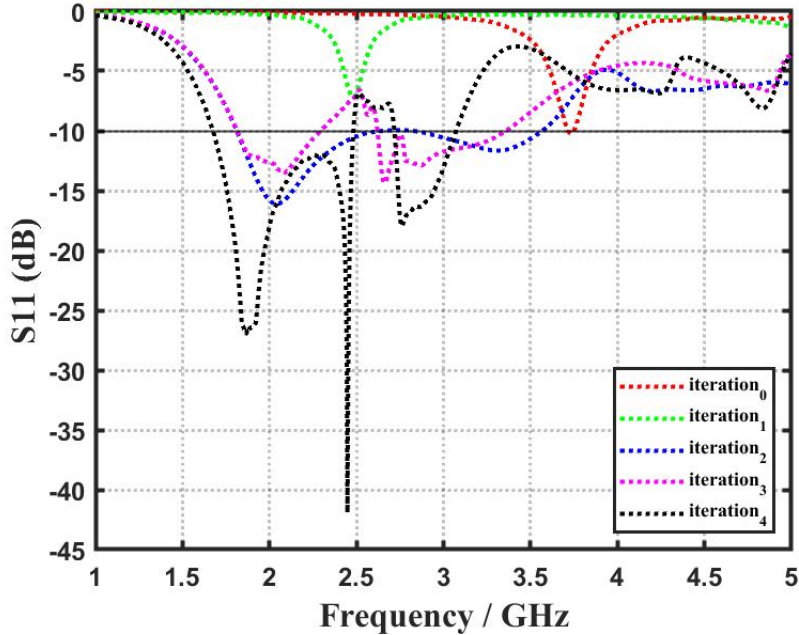


Figure 4.8: Variation of reflection coefficient (S11) of Antenna Design 1 with iterations

gain of 3.66 dBi. The antenna was further modified in iteration 4 as shown in figure 4.6e and 4.7e by etching a horizontal rectangular slot and two small slots beside the feed the patch. The ground plane was modified by adding copper between and adjacent to the split rings. These slots contributed to an increase in capacitance and electrical length of the antenna, resulting in the antenna resonating at the desired frequency.

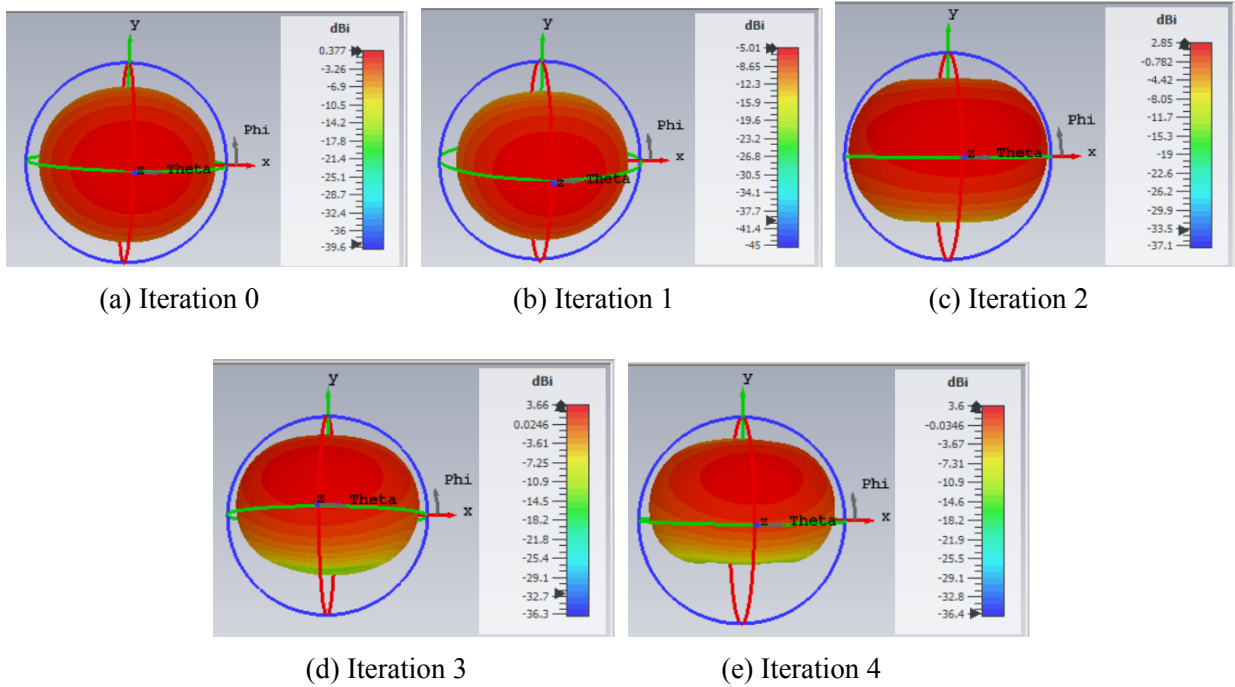


Figure 4.9: Variation of radiation pattern (gain) of antenna from iteration 0 to iteration 4

In iteration 4, antenna resonated at 2.45 GHz with a -10 dB bandwidth from 1.68 GHz to 2.48 GHz having S11 equal to -40 dB at 2.45 GHz. The antenna had a fractional bandwidth and a peak gain of 38.5% and 3.6 dBi. The overall dimensions of the proposed antenna are 36 mm x 55 mm x 0.6 mm ($0.29\lambda_o$ mm x $0.45\lambda_o$ mm x $0.005\lambda_o$ mm). The design evolution steps of the patch and ground plane, along with their corresponding S11 and gain of the antenna, are illustrated in Figures 4.6, 4.7, 4.8 and 4.9 respectively. Figures 4.10a and 4.10b exhibit the superior top and bottom views of the proposed antenna, respectively. After its ultimate iteration, the optimized parameters of the antenna are enumerated in Table 4.2. Figures 4.10c, 4.10d, and 4.10e aptly showcase the surface current density of the antenna at the 2.45 GHz frequency.

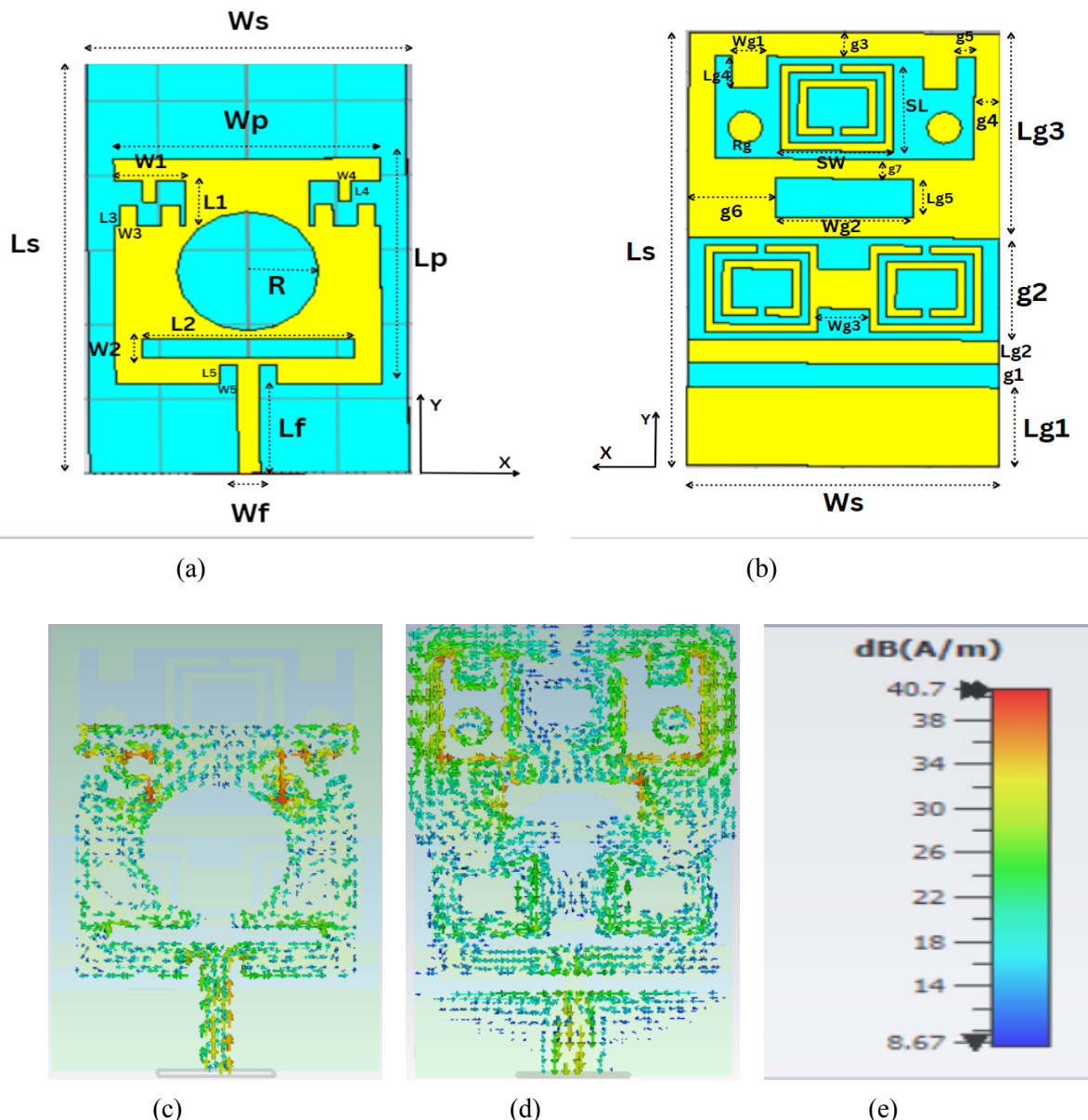


Figure 4.10: Topology of final proposed antenna: (a) top view, (b) bottom view and surface current distribution of the antenna at 2.45GHz (c), (d), (e)

Table 4.2
Optimized design parameters of proposed antenna in Figure 4.10a and 4.10b

Dimensions (unit: mm)						
Ws = 36	Ls = 55	Wp = 30	Lp = 30.25	Wf = 2.5	Lf = 12	W1 = 8
L1 = 6	W2 = 2.5	L2 = 24	W3 = 2	L3 = 2.8	W4 = 1.5	L4 = 2.8
W5 = 2	L5 = 2.5	R = 8	Lg1 = 10	Lg2 = 3	Lg3 = 26	Lg4 = 4
Lg5 = 5	Wg1 = 4	Wg2 = 16	Wg3 = 6	g1 = 3	g2 = 13	g3 = 3
g4 = 3	g5 = 2	g6 = 10	g7 = 2.5	SL = 11	SW = 13	Rg = 2
h = 0.5				t = 0.05		

Section 5.1.2 of chapter 5 delved into the performance of antenna design 2. While the antenna does satisfy the essential performance criteria for the WBAN, there is still an opportunity to enhance its size and radiation efficiency. This drive for improvement has led us to put forth an alternative antenna design.

4.1.3 Antenna Design 3

The design process started by designing a conventional patch antenna with full ground plane fed via a microstrip line as seen in fig 4.11a, 4.12a and the measured gain and S11 were 0.1115 dBi and -9.1667 dB resonating at 3.775 Ghz, respectively. This is iteration 0,

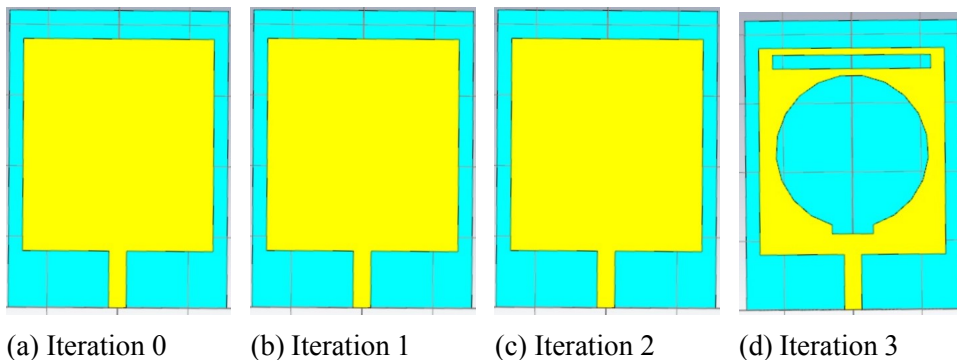


Figure 4.11: Evolution of patch of Antenna from iteration 0 to iteration 3

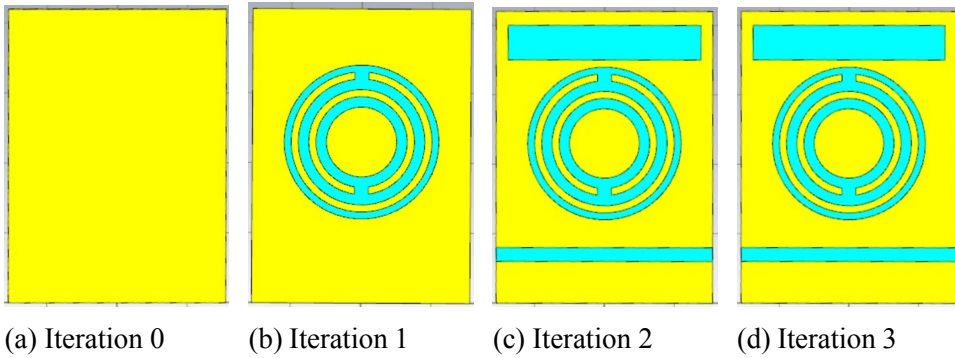


Figure 4.12: Evolution of ground plane of Antenna from iteration 0 to iteration 3

The antenna's capacitance has to be raised in order to change its resonance frequency from 3.775 Ghz to 2.45 Ghz. So in iteration 1 as shown in figures 4.11a and 4.12b Split Ring Resonators (SSRs) are introduced in the patch antenna's ground plane. The inner ring's split gap introduces a capacitance that may be exploited to modify the structure's resonance frequency. Therefore, when the circuit's capacitance rises, the resonance frequency decreases to 2.455 Ghz. S11 and gain have corresponding values of -8.806 dB and 1.837 dBi. Now the aim is to increase the gain of the antenna. So in iteration 2 As shown in figures 4.11c and 4.12c, two rectangular slots have been added to the patch antenna's ground to boost its gain and S11. Although the resonance frequency has subsequently migrated to 2.781 GHz, the antenna's gain and S11 rose to 2.576 dBi and -15.827 dB as a result of the addition of these slots. Now we have achieved desirable gain but the antenna is not resonating at our desired frequency. In iteration 3 as shown in figures 4.11d and 4.12d in order to enhance the patch antenna's electrical length and achieve the required resonance frequency, slots have been added to the patch. The patch antenna's electrical length was extended by the insertion of two rectangular slots and one circular slot, which in turn lowered the resonance frequency to the desired frequency of 2.452 GHz. Gain and S11 of the developed antenna design are 2.627 dBi and -41.723 dB, respectively.

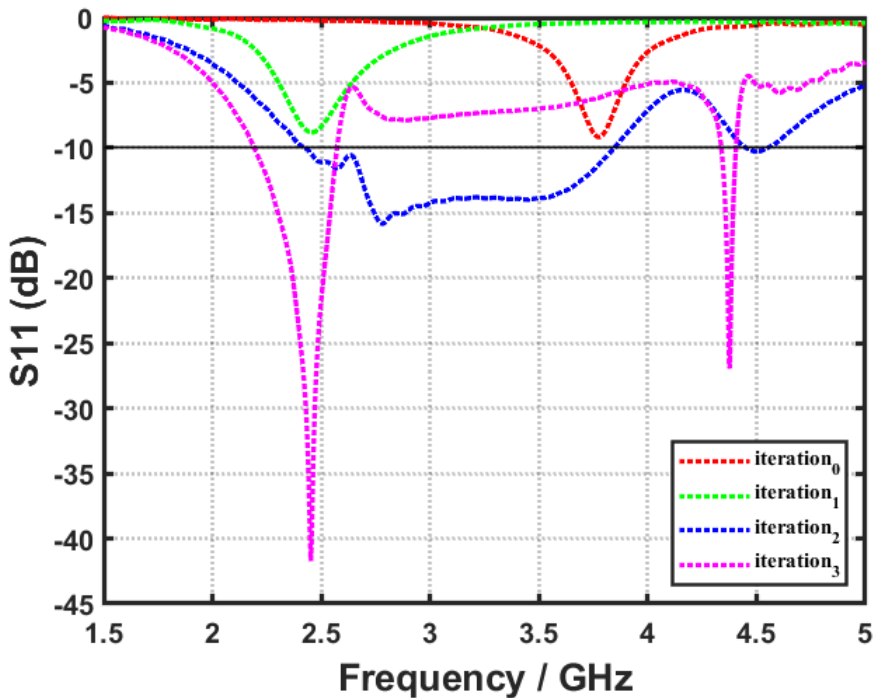


Figure 4.13: Variation of reflection coefficient (S11) of Antenna Design with iterations

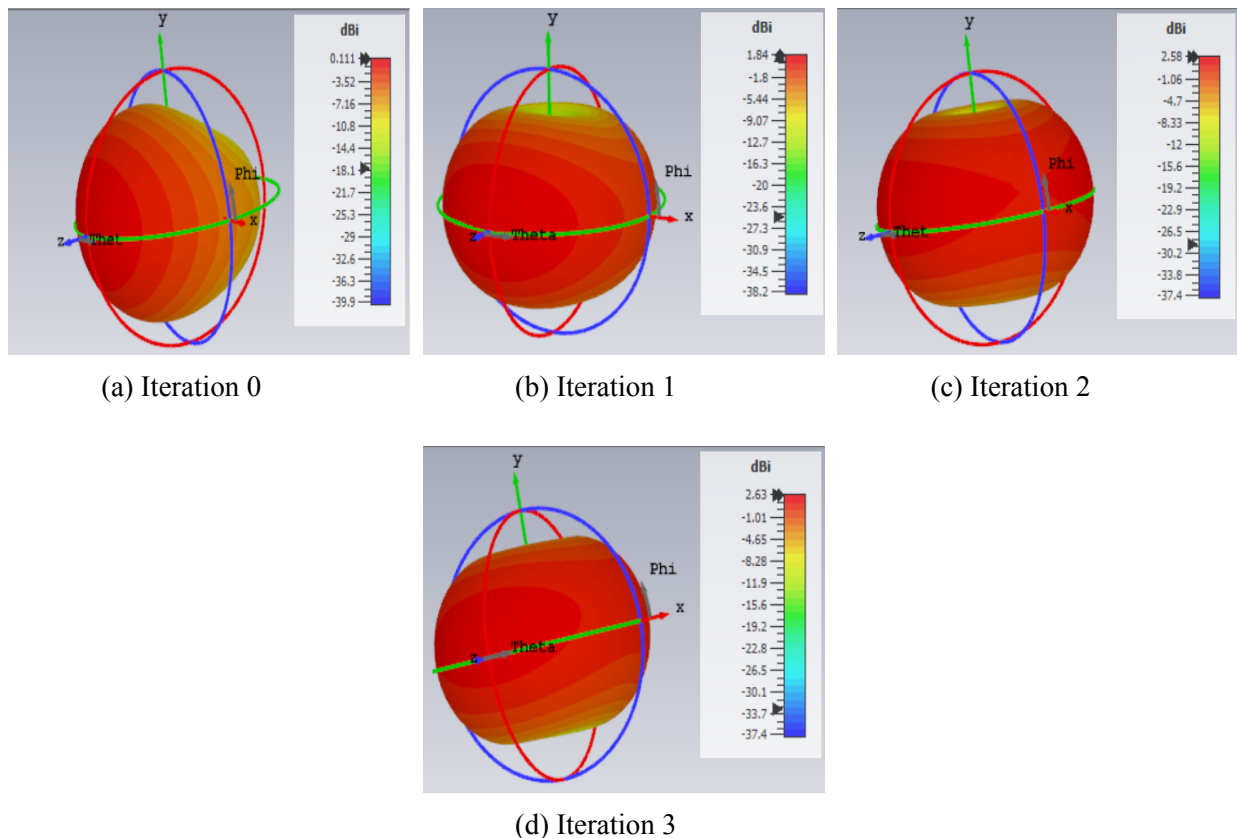


Figure 4.14: Variation of radiation pattern (gain) of antenna from iteration 0 to iteration 3

In final iteration i.e. iteration 3, antenna resonated at 2.45 GHz with a -10 dB bandwidth from 2.192

GHz to 2.571 GHz having S11 equal to -41.72 dB at 2.45 GHz. The antenna had a fractional bandwidth and a peak gain of 15.9% and 2.62 dBi. The overall dimensions of the proposed antenna are 31 mm x 42 mm x 0.6 mm ($0.25\lambda_o$ mm x $0.34\lambda_o$ mm x $0.005\lambda_o$ mm). The design evolution steps of the patch and ground plane, along with their corresponding S11 and gain of the antenna, are illustrated in Figures 4.6, 4.7, 4.8 and 4.9 respectively. Figures 4.15a and 4.15b exhibit the superior top and bottom views of the proposed antenna respectively. After its ultimate iteration, the optimized parameters of the antenna are enumerated in Table 4.3.

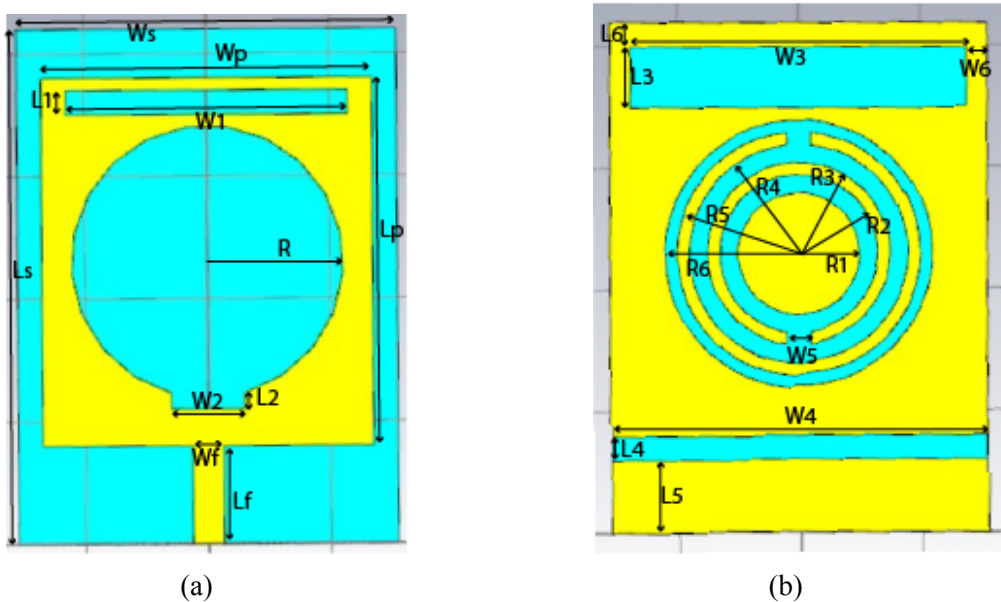


Figure 4.15: Topology of final proposed antenna: (a) top view, (b) bottom view

Table 4.3
Optimized design parameters of proposed antenna in Figure 4.10(a) and 4.10(b)

Dimensions (unit: mm)						
Ws = 31	Ls = 42	Wp = 27	Lp = 30	Wf = 2.5	Lf = 8	W1 = 23
L1 = 2	W2 = 6	L2 = 1.5	W3 = 27.6	L3 = 5	W4 = 31	L4 = 2
W5 = 2	L5 = 6	W6 = 1.7	L6 = 2	R = 11.1	R1 = 5	R2 = 6.5
R3 = 7.5	R4 = 9	R5 = 10	R6 = 11	t = 0.05		h = 0.5

In chapter 5, section 5.1.3, we explored the performance of antenna design 3 and its characteristics.

Chapter 5

RESULTS AND DISCUSSION

This chapter focuses on presenting the results and evaluating the performance of the proposed antenna designs. It also conducts a comparative analysis of the proposed antennas with existing wearable antennas.

5.1 Performance Analysis of Proposed Antenna Designs

The antennas were simulated using the Computer Simulation Technology (CST) software. The investigation of proposed antenna's on-body performance was conducted by establishing a three-layer human tissue phantom model measuring 30 mm x 45 mm x 5.5 mm in CST Microwave Studio, as illustrated in Figure 5.1. The details of the phantom model are listed in Table 5.1.

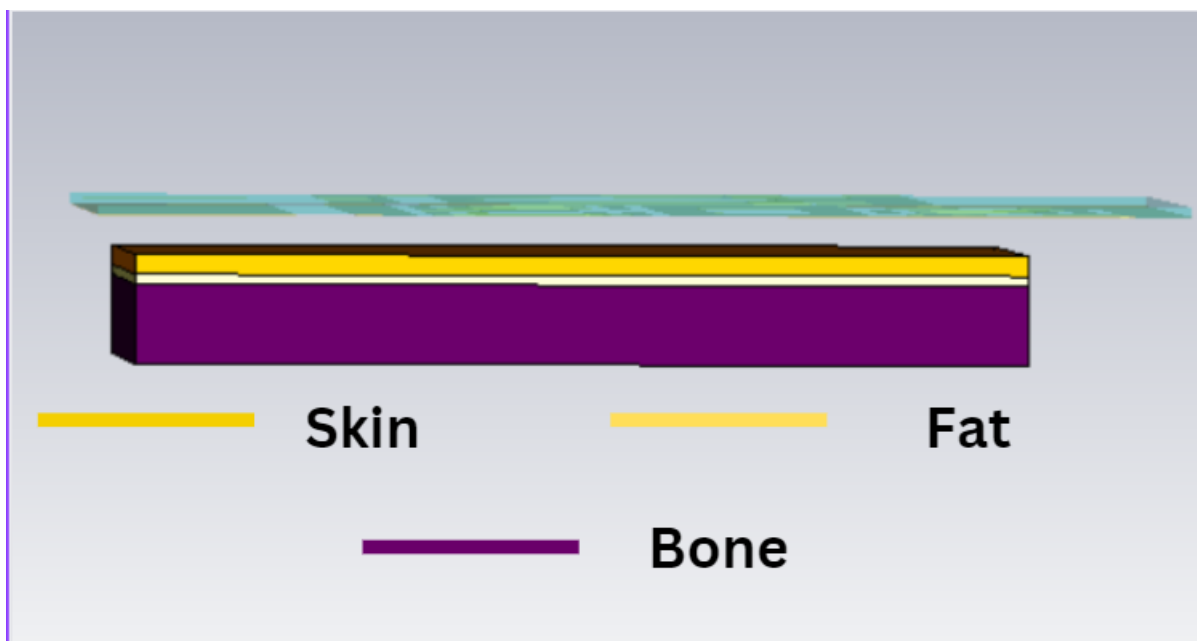


Figure 5.1: Human tissue phantom model

Table 5.1
Properties of human tissue phantom model

Tissue	Skin	Fat	Bone
Dielectric Constant (ϵ)	36.6	10.4	16.9
Conductivity [σ (S/m)]	2.34	0.502	1.4
Density [ρ (kg/m³)]	1060	900	1300
Thickness (mm)	1	0.5	4

5.1.1 Antenna Design 1

Figures 5.2a and 5.2b show the fabricated antenna. The proposed antenna was tested using the VNA (Vector Network Analysis).

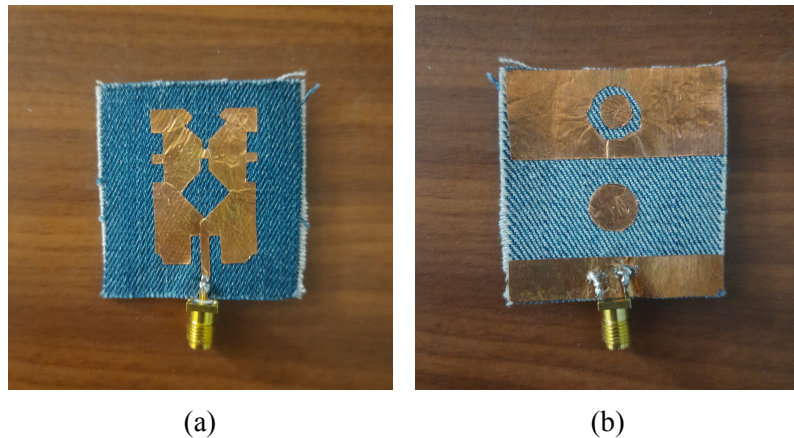


Figure 5.2: Fabricated proposed antenna (a) top view and (b) bottom view

5.1.1.1 S11 Parameter

Simulation results give us S11 as -29.225 dB at 2.45 GHz frequency with a -10dB impedance bandwidth of 1.014 GHz(1.895 GHz to 2.909 GHz) and a fractional bandwidth 42.21%. When the simulation is run with the phantom model S11 is -16.79 at 2.45 GHz with a -10 dB impedance bandwidth of 0.875 GHz (2.0315 to 2.9064 GHz) with a fractional bandwidth of 35.44%. The observed differences in all the values can be attributed to human errors, extra materials used during fabrication and jagged edges of the jeans substrate. Figure 5.3 illustrates the simulated results of S11 and Figure 5.4 illustrates the results of S11 in the presence of the phantom model.

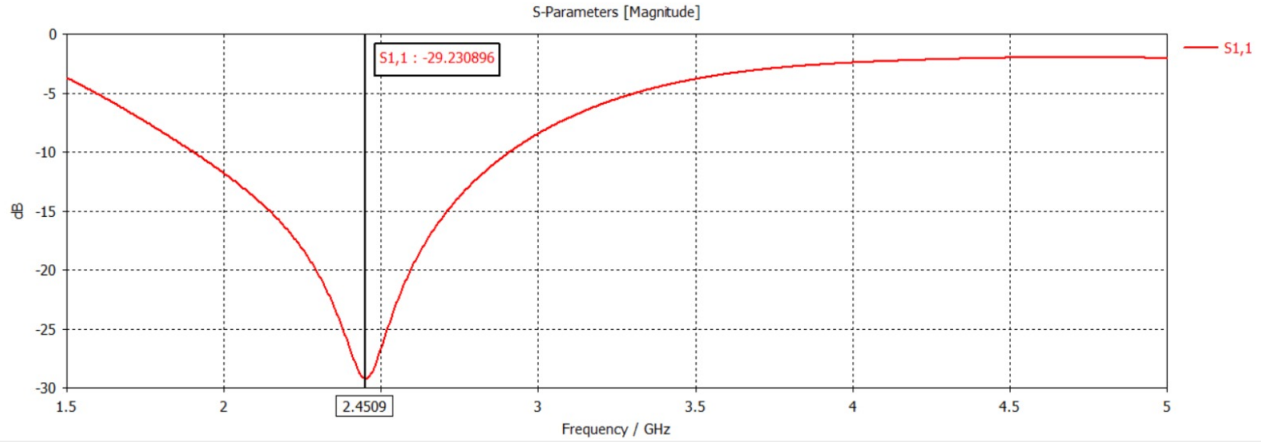


Figure 5.3: Simulated S11 of the proposed antenna

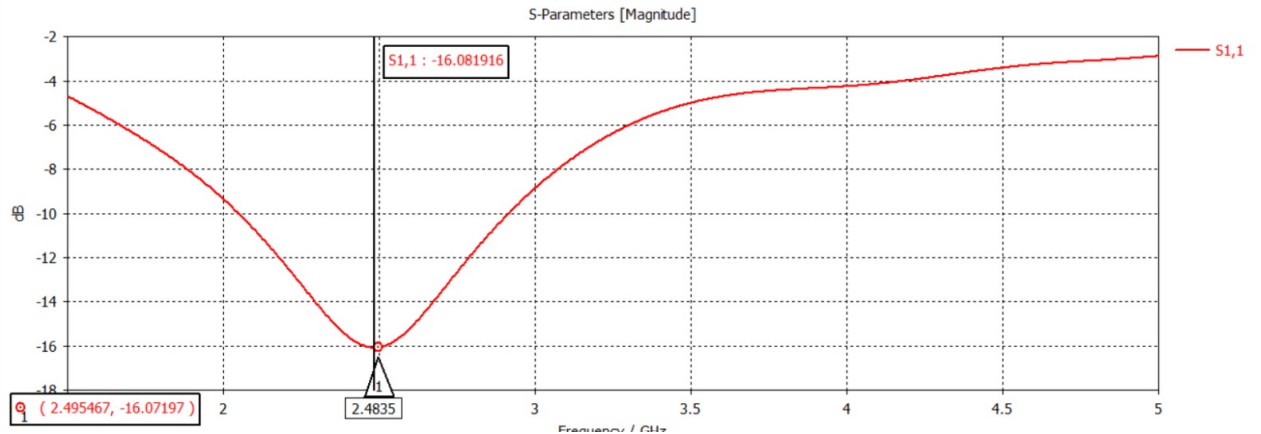


Figure 5.4: S11 results of the proposed antenna with phantom model

5.1.1.2 Gain and radiation Efficiency

Simulation of the antenna gives us a maximum gain of 1.828 dBi with a radiation efficiency of 86.27% as shown in Figure 5.5. Figures 5.6a and 5.6b demonstrate the antenna radiation patterns in the E-plane ($\phi = 0^\circ$) and H-plane ($\phi = 90^\circ$) respectively. Figures 5.7a and 5.7b demonstrate the antenna radiation patterns in the E-plane ($\phi = 0^\circ$) and H-plane ($\phi = 90^\circ$) respectively in the presence of phantom model.

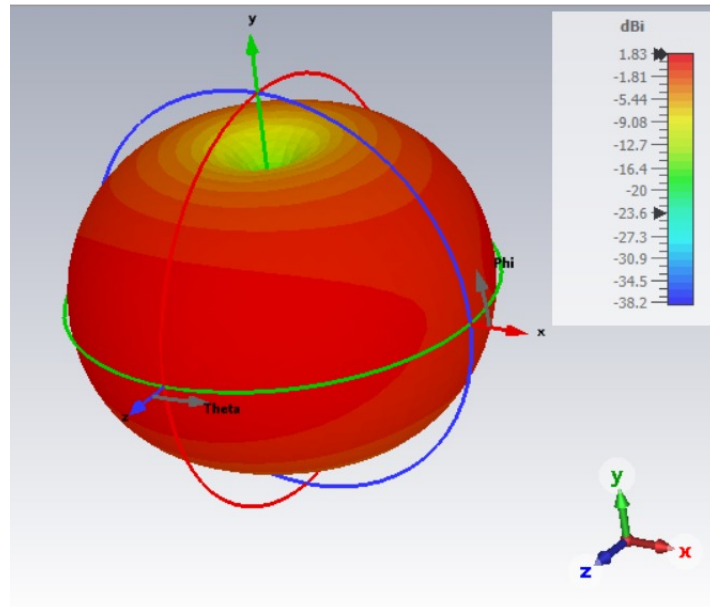


Figure 5.5: Gain of the proposed antenna

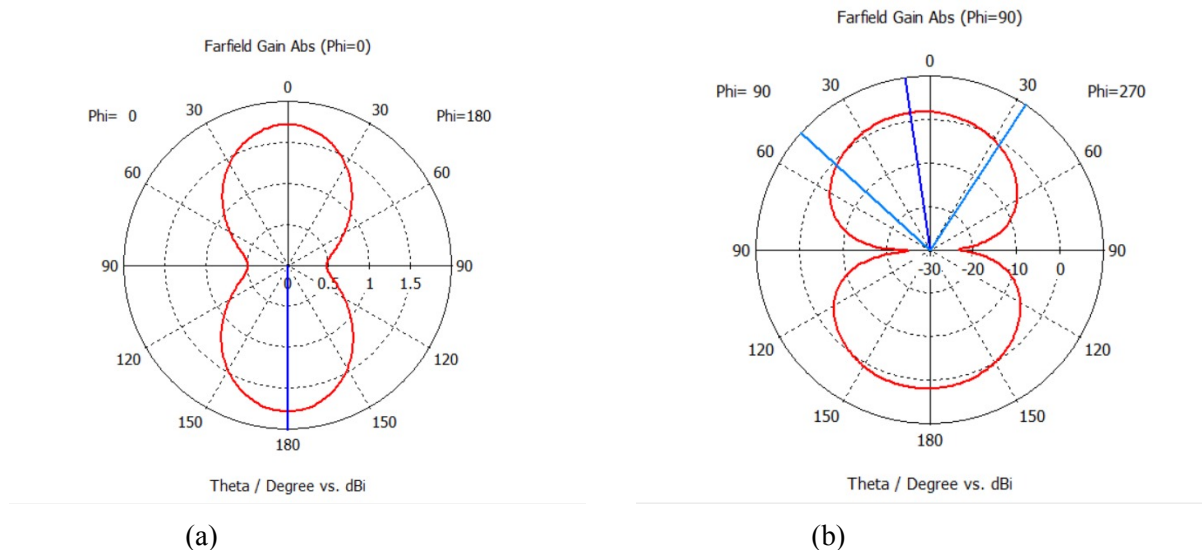


Figure 5.6: Simulated radiation patterns of the proposed antenna in the (a) E-plane ($\phi = 0^\circ$) and (b) H-plane ($\phi = 90^\circ$)

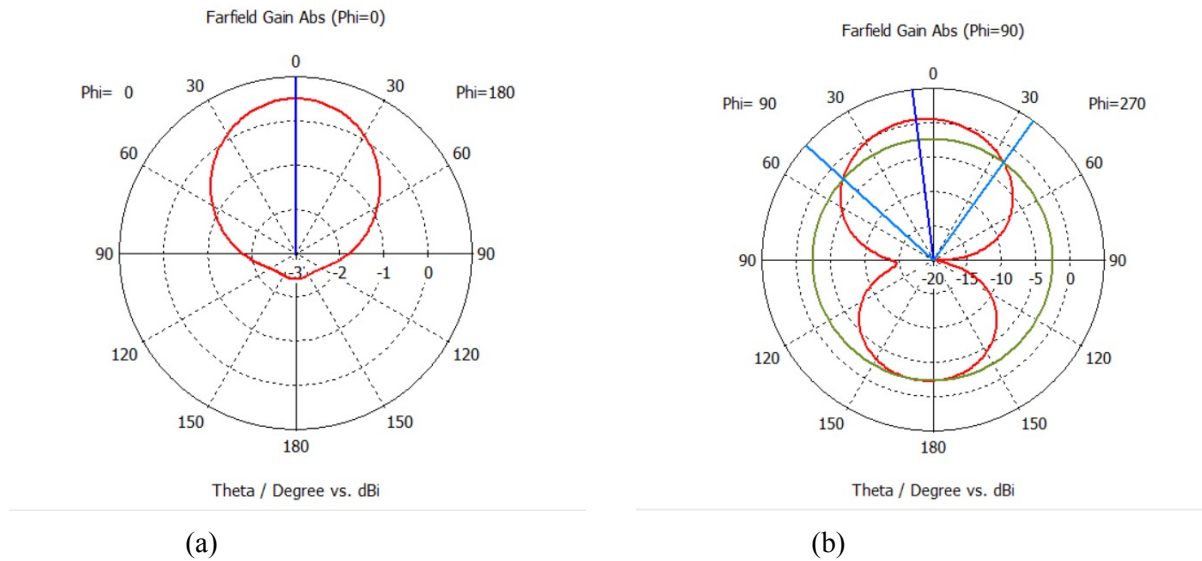


Figure 5.7: Simulated(with phantom model) radiation patterns of the proposed antenna in the (a) E-plane ($\phi = 0^\circ$) and (b) H-plane ($\phi = 90^\circ$)

5.1.1.3 Specific Absorption Rate (SAR)

Since the main aim of this project is to design a flexible patch antenna which can be used in WBAN devices, the SAR for this antenna has also been calculated on a phantom model shown in Figure 5.1. The simulation was performed for 1g of tissue. Obtained SAR value is 0.05642W/Kg which is less than the limits kept by IEEE and FCC. Figure 5.8 shows the simulated results.

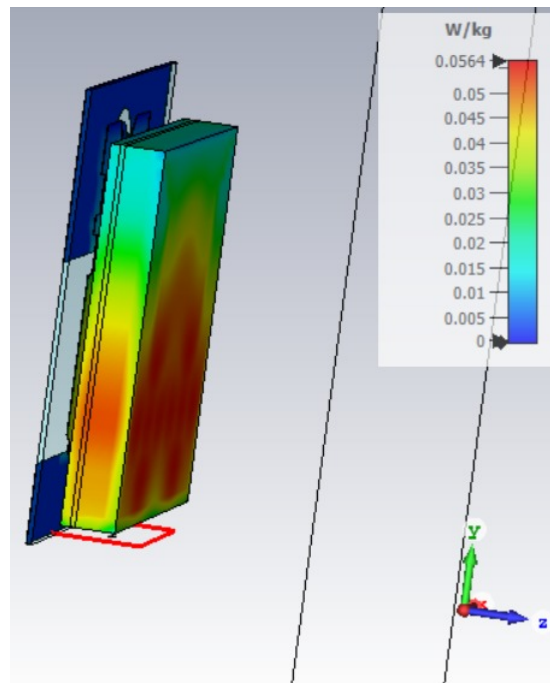


Figure 5.8: Measured SAR value of proposed antenna

5.1.2 Antenna Design 2

Figures 5.9a and 5.9b depict the fabricated antenna. The proposed antenna was tested on a Vector Network Analyzer, as shown in Figure 5.10.

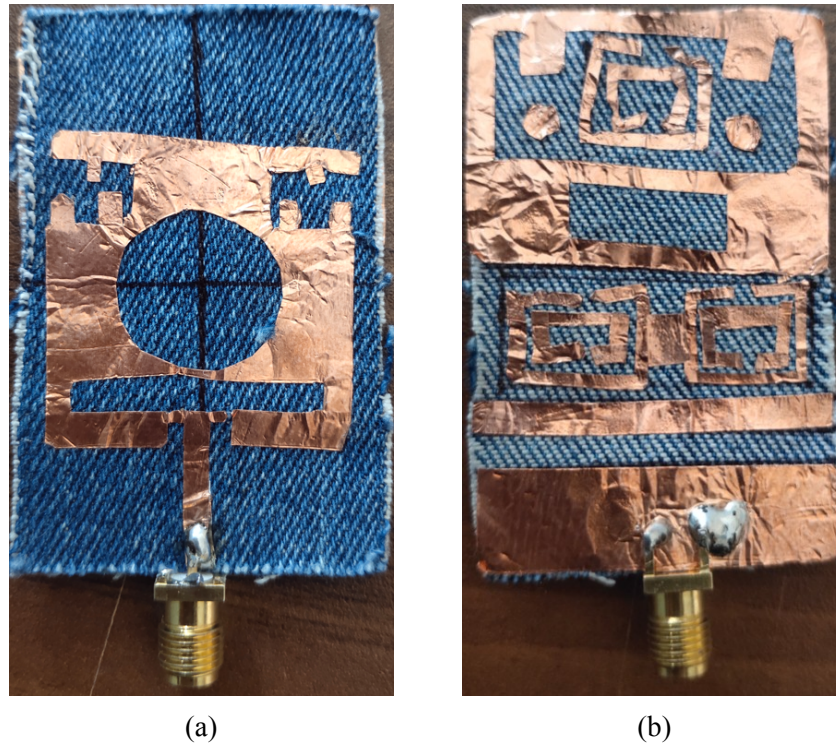


Figure 5.9: Fabricated proposed antenna (a) top view and (b) bottom view

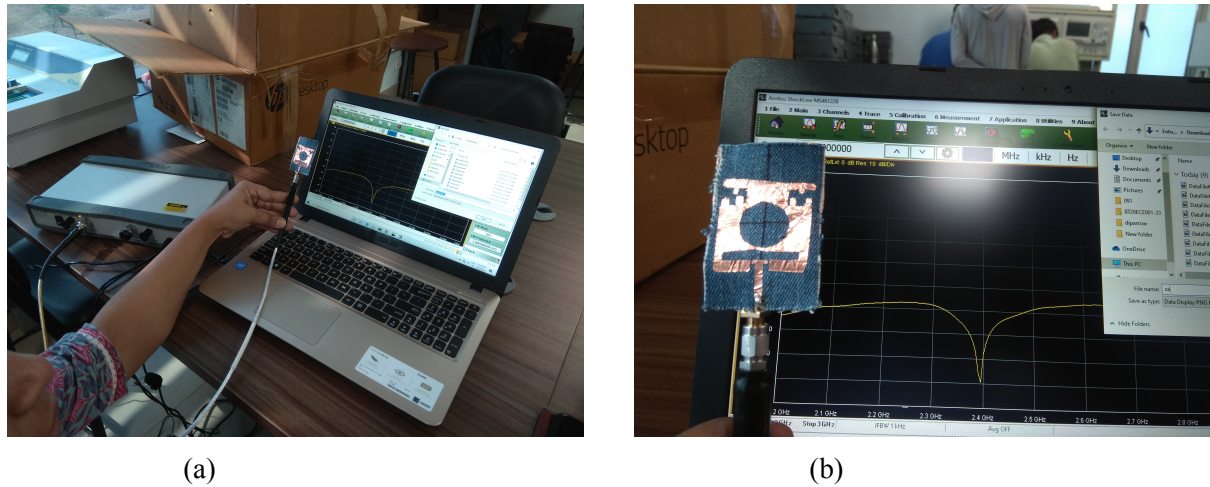


Figure 5.10: Testing of proposed antenna on VNA

5.1.2.1 S11 Parameter

Figure 5.11 illustrates the simulated, measured and human tissue phantom model S11 values of the proposed antenna. The simulated S11 at 2.45 GHz is -41 dB with a -10 dB impedance bandwidth of 0.8 GHz (1.68 GHz to 2.48 GHz) and a fractional bandwidth of 38.5%. The measured S11, while slightly differing from the simulated values, still demonstrates a band of 2.4 – 2.5 GHz, with a value of -22 dB at 2.45 GHz. The difference between these values can be attributed to fabrication and soldering errors. However, both results suggest that the proposed antenna meets the requirements of the ISM frequency band. Furthermore, the antenna was tested on a human tissue phantom model, yielding an S11 value of -17.5 dB at 2.5GHz with a -10 dB impedance bandwidth of 1.208 GHz (1.552GHz to 2.76 GHz) and a fractional bandwidth of 56%, fulfilling the necessary requirements. It's noteworthy that the S11 values of the proposed antenna on the human tissue phantom model and measured S11 values are consistent with each other.

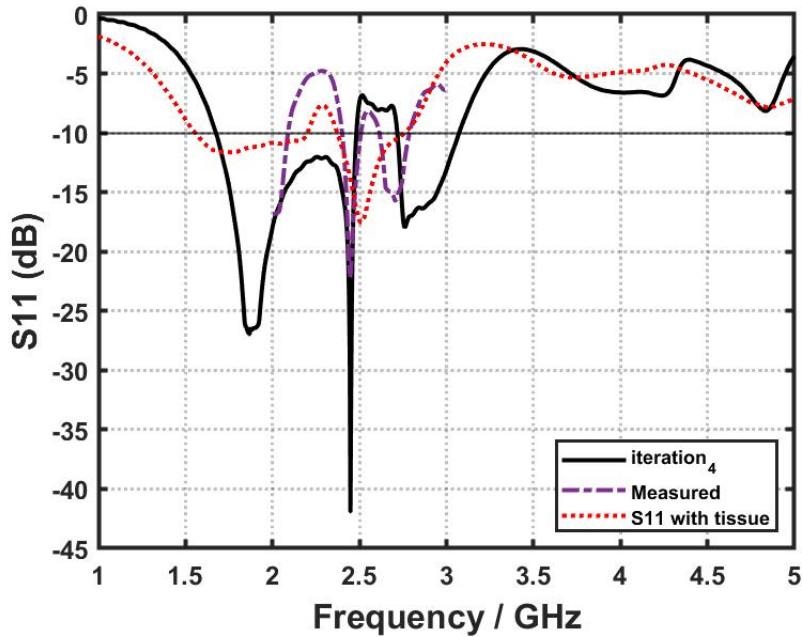


Figure 5.11: Simulated, measured and with human tissue reflection coefficient (S11) of proposed antenna

5.1.2.2 Gain and radiation Efficiency

The proposed antenna exhibited a maximum gain of 3.6 dBi at 2.45 GHz, coupled with a radiation efficiency of 77.7%, as illustrated in Figure 5.12. Both the measured and simulated gain values of the antenna demonstrated excellent concurrence. The radiation patterns of the antenna in the E-plane ($\phi = 0^\circ$) and H-plane ($\phi = 90^\circ$) were portrayed in Figures 5.13a and 5.13b, respectively, both in

simulation and measurement.

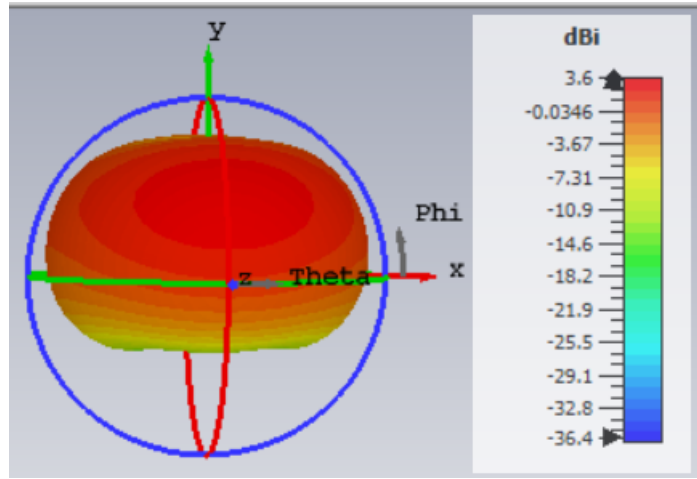


Figure 5.12: Gain of the proposed antenna

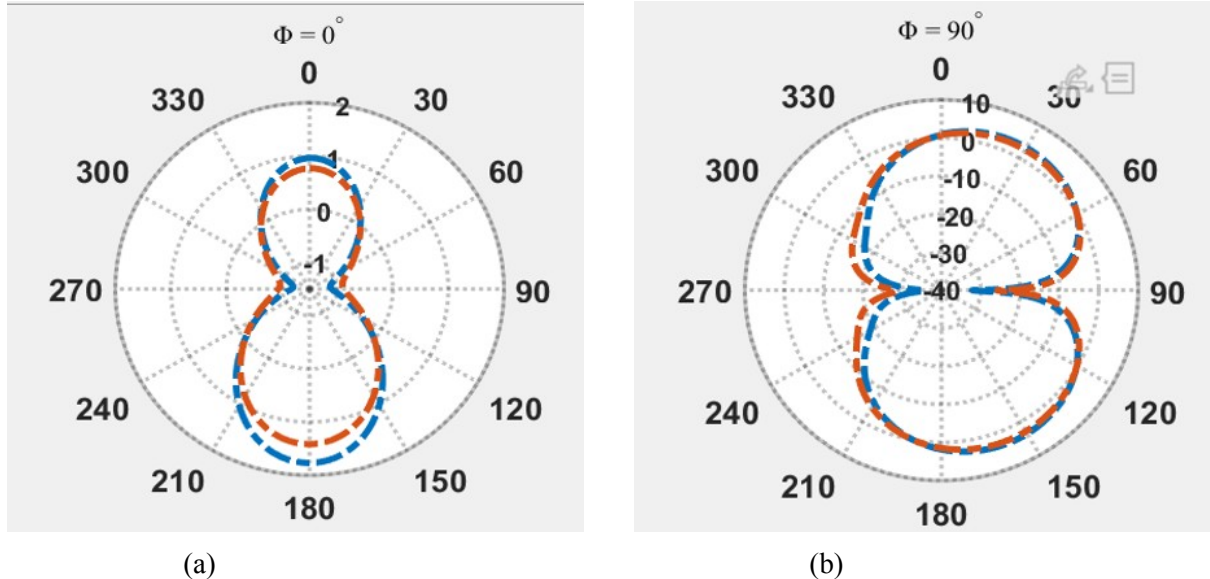


Figure 5.13: Measured and simulated radiation patterns of the proposed antenna in the (a) E-plane ($\phi = 0^\circ$) and (b) H-plane ($\phi = 90^\circ$)

5.1.2.3 Specific Absorption Rate (SAR)

It is necessary to determine the SAR prior to using any antenna in a Wireless Body Area Network (WBAN) to ensure that it complies with safety limits [24].

In order to safeguard against the potential risks of harmful radiation, regulatory restrictions have been established by the International Commission on Non-Ionizing Radiation Protection (ICNIRP). According to these guidelines, the maximum SAR value must not exceed 2.0 W/kg for 10g of tissue.

Similarly, the Federal Communications Commission (FCC) has mandated that the SAR should not exceed 1.6 W/kg for 1g of tissue.

To evaluate the suitability of the proposed antenna for on-body applications, the SAR was measured on a three-layered human tissue model shown in Figure 5.1 with a 2 mm offset between the antenna and the model, as illustrated in Figure 5.14. The SAR value was found to be 0.114 W/kg for 1g of tissue, which falls well within the limits set by the FCC and IEEE standards [25]. Based on these results, it can be concluded that the proposed antenna is well-suited for on-body use.

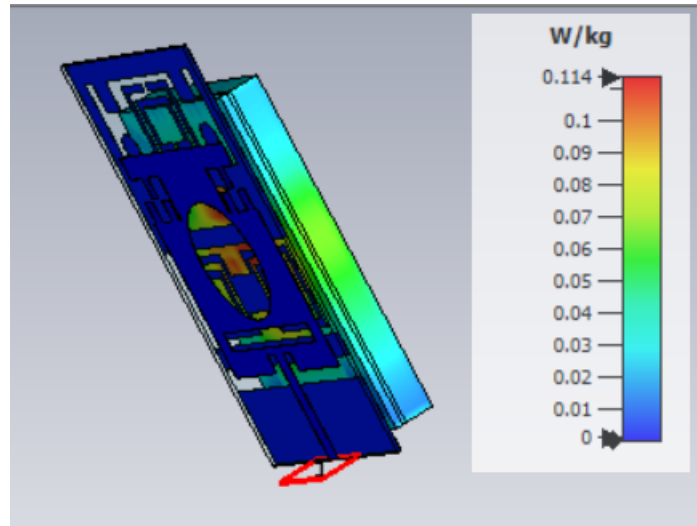


Figure 5.14: Measured SAR value of the proposed antenna

5.1.2.4 Bending Analysis

In scenarios where antennas are worn on the body, it is anticipated that they will undergo bending during use. This section presents an analysis of the antenna's performance under two bending conditions: vertical (y-axis) and horizontal (x-axis), with varying curvatures. The antenna's S11, gain, and radiation pattern were studied by analysing different radii ($R_x = 80$ mm, 40 mm, 20 mm, $R_y = 80$ mm, 40 mm, 20 mm) along the x-axis and y-axis. The proposed antenna's structure, S11, and radiation patterns under different bending conditions in the x-axis and y-axis are illustrated in figures 5.15, 5.16, 5.17 and 5.18, respectively.

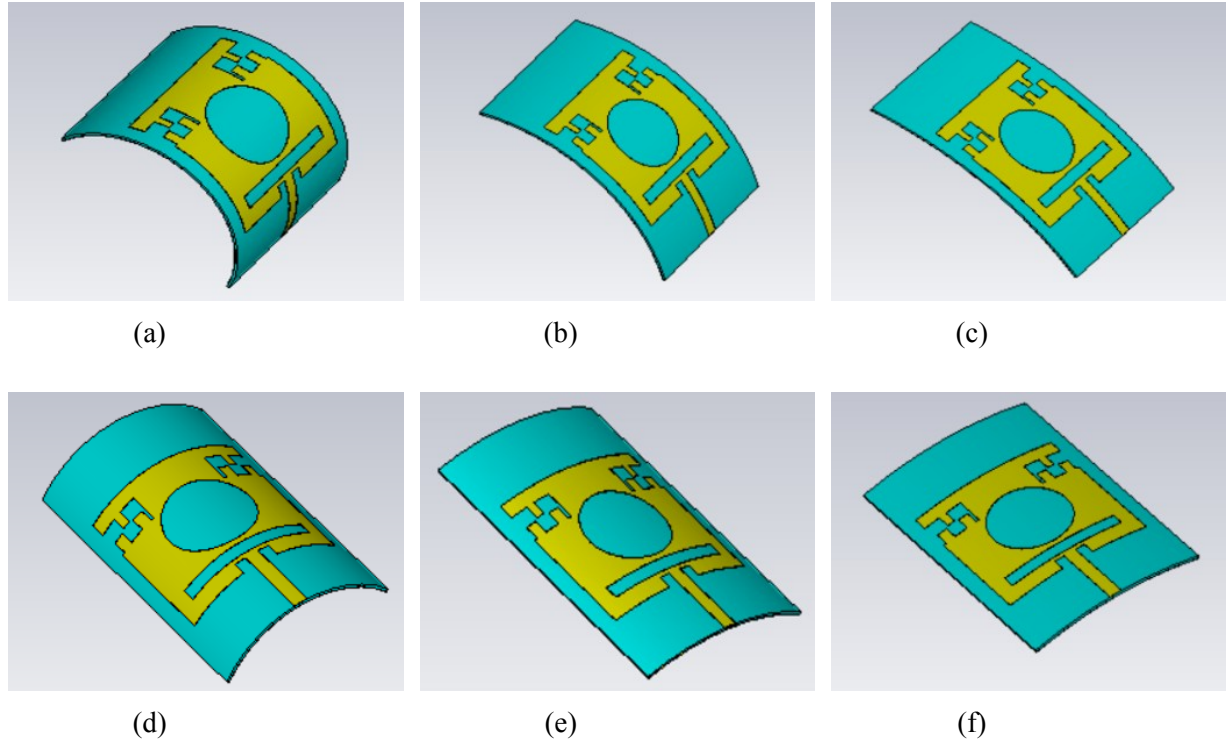


Figure 5.15: Structure of antenna under two bending condition with different radii, horizontal (x-axis) (a) $R_x = 20$ mm, (b) $R_x = 40$ mm, (c) $R_x = 80$ mm and Vertical (y-axis) (d) $R_y = 20$ mm, (e) $R_y = 40$ mm, (f) $R_x = 80$ mm

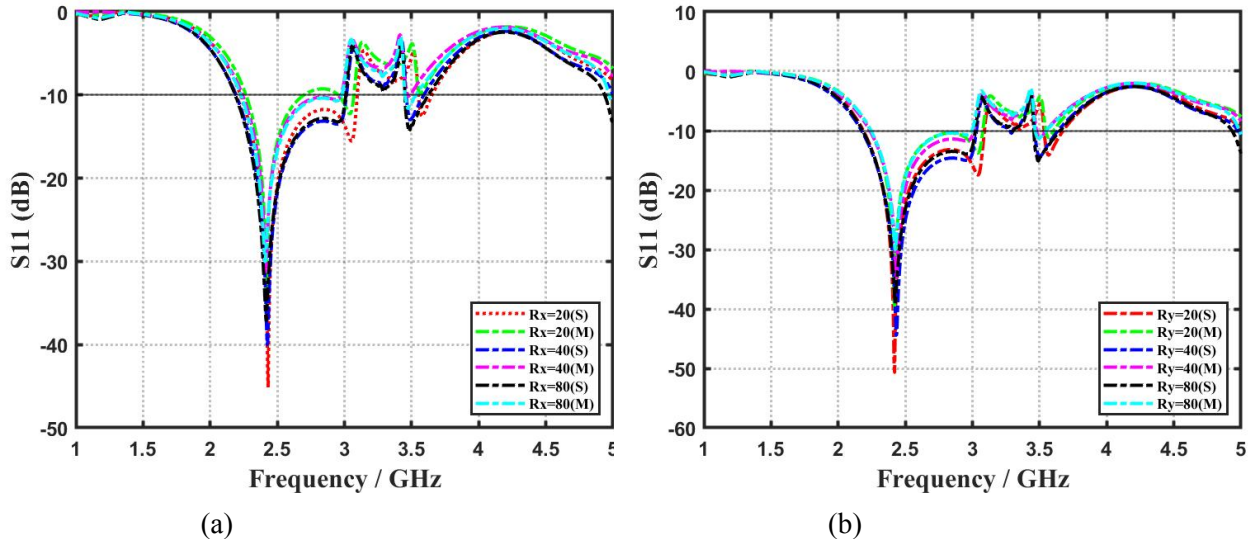


Figure 5.16: Measured and simulated $S_{11}(s)$ of the proposed antenna under (a) horizontal (x-axis) and (b) vertical (y-axis) bending conditions with different curvatures

The resonance frequency for all bending scenarios exhibited minimal change, indicating that the antenna's performance is not significantly affected by bending. Moreover, the radiation patterns of the antenna remained undistorted under bending scenarios at 2.45 GHz. The antenna's gain improved

under the bending scenarios. Under all bending conditions, the antenna was well-matched at the targeted ISM (2.45) band. Based on this study, the proposed antenna has the potential to be utilized in applications where bending may occur. Table 5.2 provides a comprehensive comparison of the antenna's performance in both unbent and bent conditions. Additionally, the study concludes that the proposed antenna is flexible.

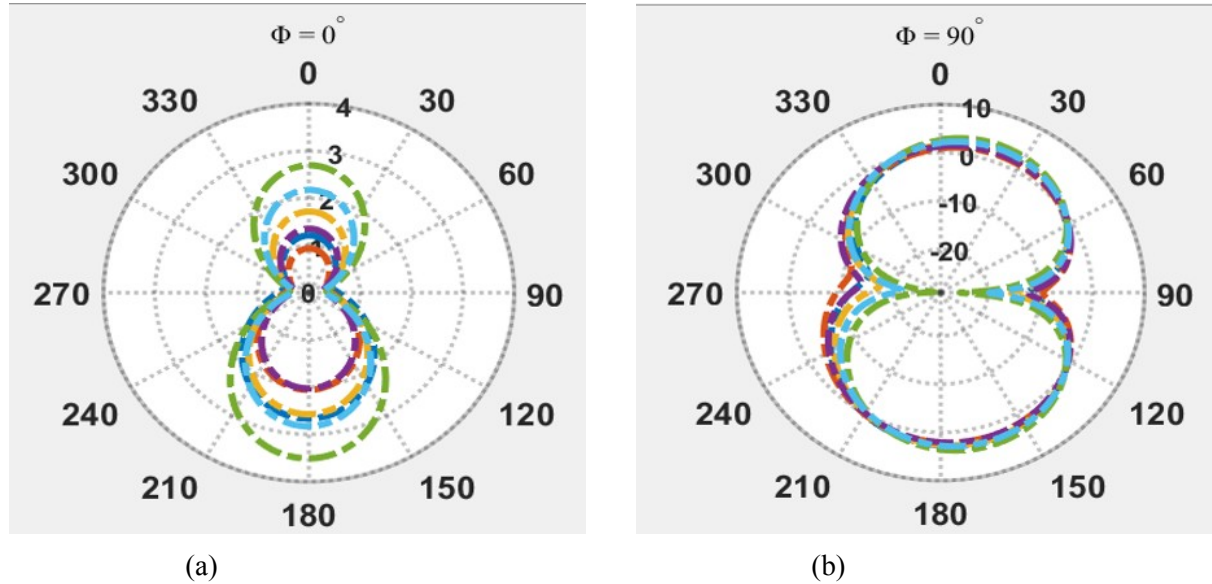


Figure 5.17: Measured and simulated radiation patterns of the proposed antenna under horizontal (x-axis) bending condition in the (a) E-plane ($\phi = 0^\circ$) and (b) H-plane ($\phi = 90^\circ$)

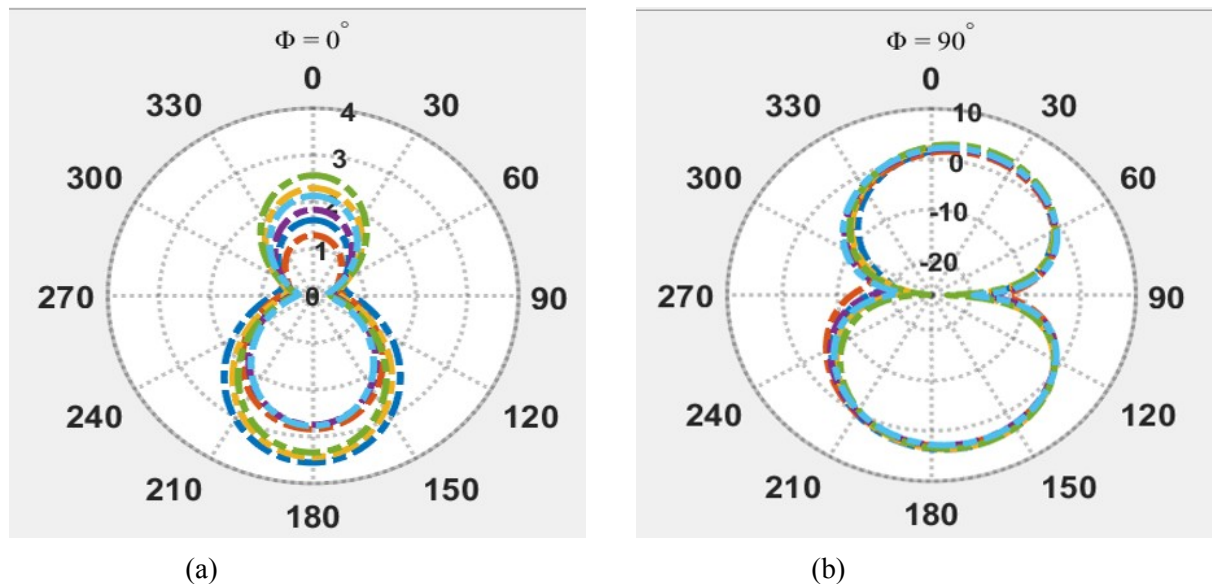


Figure 5.18: Measured and simulated radiation patterns of the proposed antenna under vertical (y-axis) bending condition in the (a) E-plane ($\phi = 0^\circ$) and (b) H-plane ($\phi = 90^\circ$)

Table 5.2
Comparison of antenna properties under two bending conditions with different curvatures

Bending in x-axis (Horizontal)				Bending in y-axis (Vertical)			
R_x (mm)	Res. freq (GHz)	S11 (dB)	Gain (dBi)	R_y (mm)	Res. freq (GHz)	S11 (dB)	Gain (dBi)
Unbent	2.45	-41	3.6	Unbent	2.45	-41	3.6
20	2.43	-45.14	3.84	20	2.42	-50	3.94
40	2.424	-40	3.78	40	2.43	-44.5	3.89
80	2.415	-37.13	3.82	80	2.424	-39	3.9

5.1.3 Antenna Design 3

Figures 5.19a and 5.19b depict the fabricated antenna. As shown in Figure 5.20, the proposed antenna was tested using a vector network analyzer.

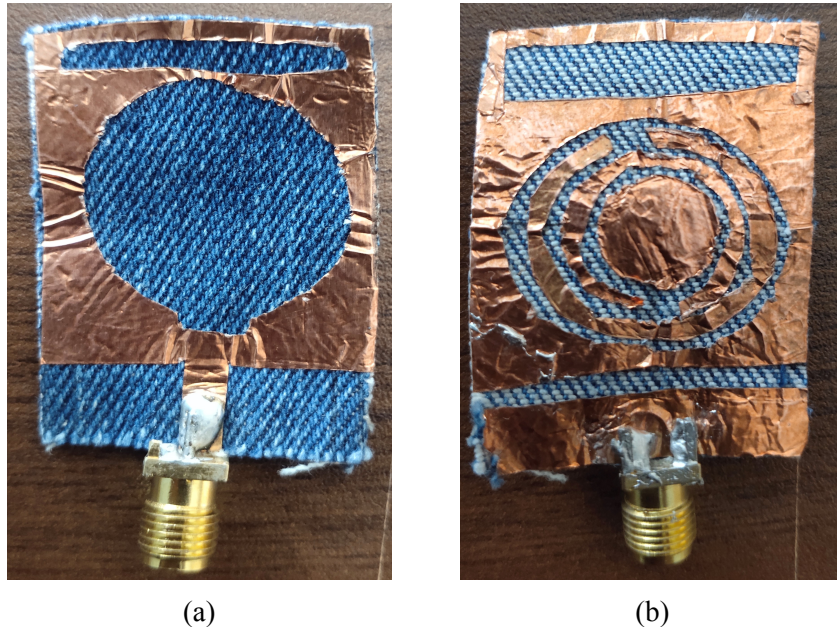


Figure 5.19: Fabricated proposed antenna (a) top view and (b) bottom view

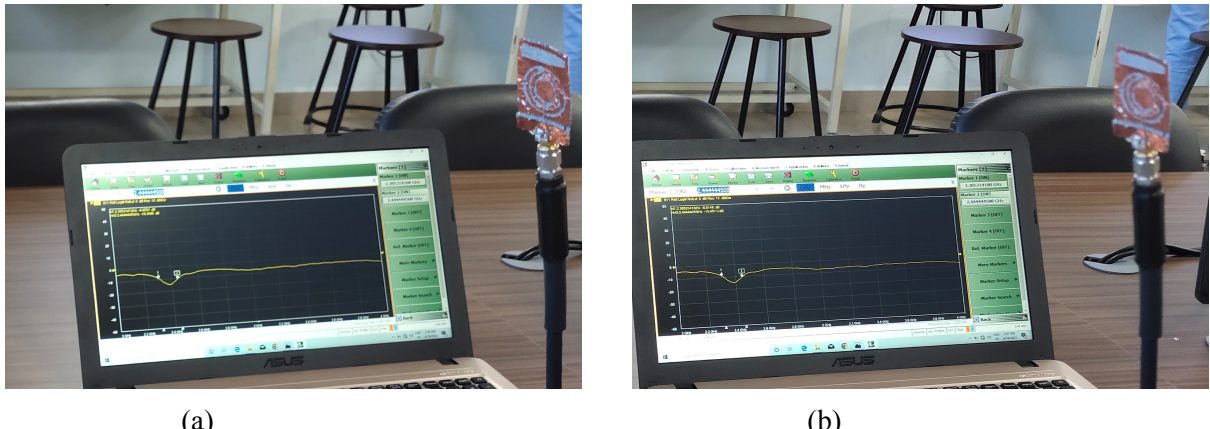


Figure 5.20: Testing of the proposed antenna on VNA

5.1.3.1 S11 Parameter

As shown in Figure 5.21 the measured S11 slightly varied from the simulated (expected) results which were caused by manufacturing errors such as jagged edges as well as extra metal used during soldering. The S11 simulation results revealed that the antenna is resonating at 2.45 GHz with a reflection coefficient of -41.72, a -10 dB impedance bandwidth of 0.379 GHz (2.192 GHz to 2.571 GHz), and a fractional bandwidth of 15.9%. When simulated using a phantom model simulation revealed that the antenna is resonating at 2.45 GHz with a reflection coefficient of -40, a -10 dB impedance bandwidth of 0.4054 GHz (2.1322 GHz to 2.5376 GHz), and a fractional bandwidth of 17.36%.

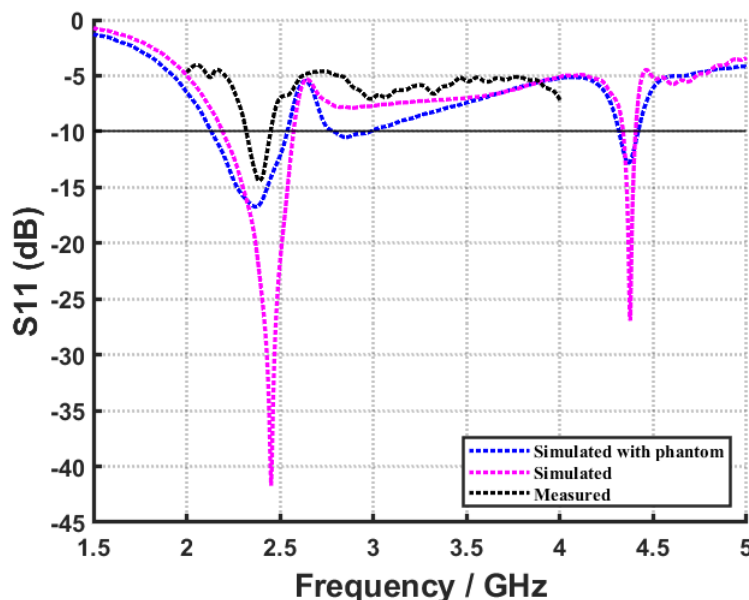


Figure 5.21: Simulated, measured and with human tissue reflection coefficient (S11) of proposed antenna

The fact that the measured results and the simulated results (with and without the phantom model) are in accordance with one another suggests that the designed antenna is suitable for application in the ISM frequency band.

5.1.3.2 Gain and radiation Efficiency

The proposed antenna exhibited a maximum gain of 2.627 dBi at 2.45 GHz, coupled with a radiation efficiency of 90.86%, as illustrated in Figure 5.22. Both the simulated(with phantom) and simulated(without phantom) gain values of the antenna demonstrated excellent concurrence. The radiation patterns of the antenna in the E-plane ($\phi = 0^\circ$) and H-plane ($\phi = 90^\circ$) were portrayed in Figures 5.23 and 5.24, respectively, both without and with phantom model.

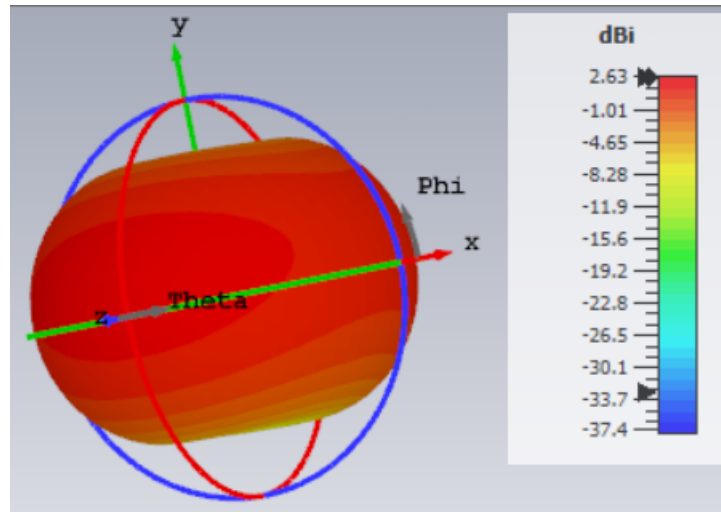


Figure 5.22: Gain of the proposed antenna

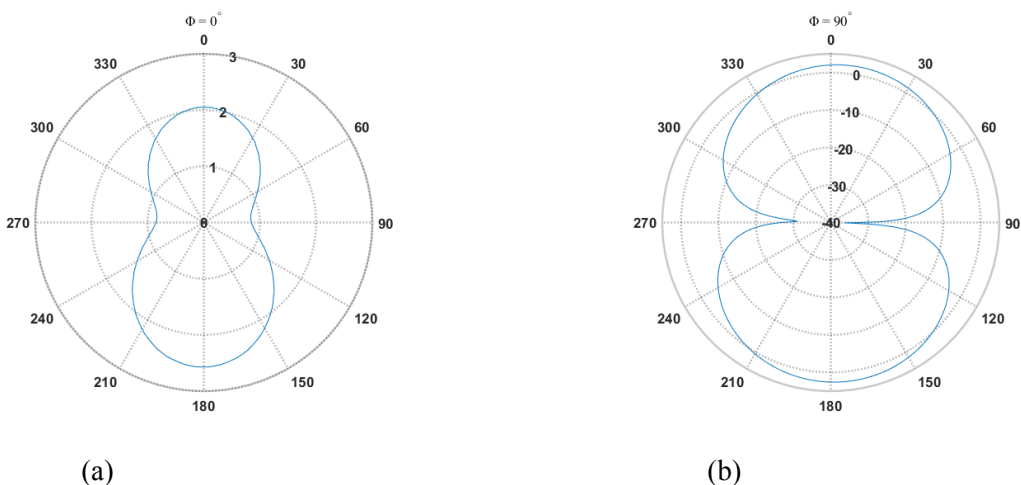


Figure 5.23: Simulated radiation patterns of the proposed antenna in the (a) E-plane ($\phi = 0^\circ$) and (b) H-plane ($\phi = 90^\circ$)

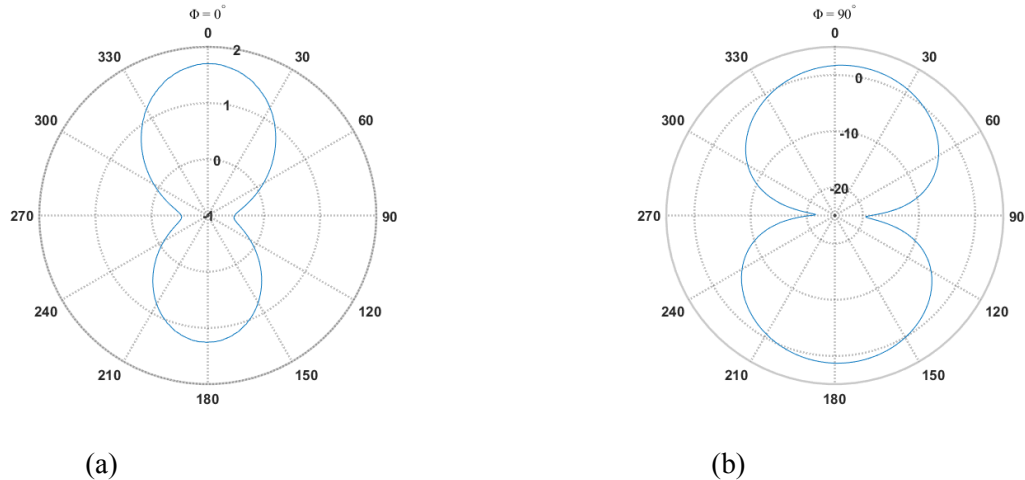


Figure 5.24: Simulated(with phantom model) radiation patterns of the proposed antenna in the (a) E-plane ($\phi = 0^\circ$) and (b) H-plane ($\phi = 90^\circ$)

5.1.3.3 Specific Absorption Rate (SAR)

On the phantom model as shown in Figure 5.1, the antenna was simulated for 1 g of tissue. The SAR value obtained is 0.0548w/kg which is considerably below acceptable safety limits suggesting that the proposed antenna is suitable for on-body applications. The simulated results for SAR are displayed in Figure 5.25.

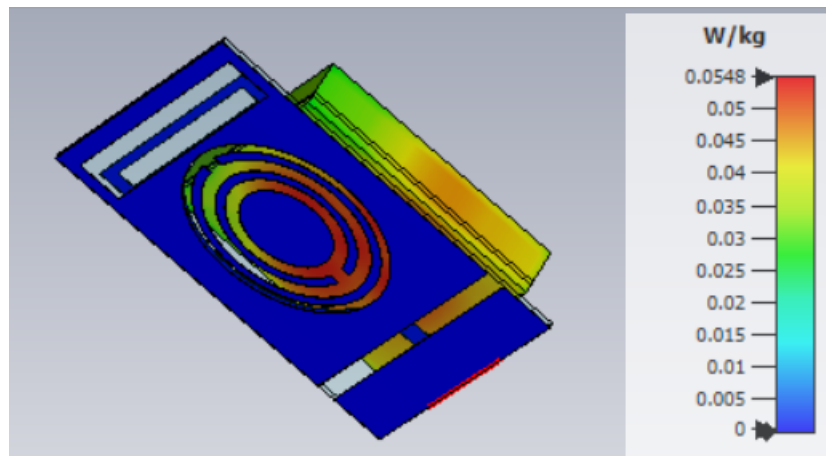


Figure 5.25: Measured SAR Value of the antenna

5.1.3.4 Bending Analysis

Wearable flexible antennas must undergo bending analysis because mechanical deformation brought on by bending or flexing might impair the antenna's electrical performance. Wearing an antenna can modify its resonance frequency, radiation pattern, and impedance matching because it is subjected to a variety of mechanical deformations. In order to do the bending analysis of the antenna, it is bent

both horizontally (along the x-axis) and vertically (along the y-axis), with a varied radius of curvature in each instance ($R_x = 80$ mm, 40 mm, 20 mm, $R_y = 80$ mm, 40 mm, 20 mm) as shown in Figure 5.26.

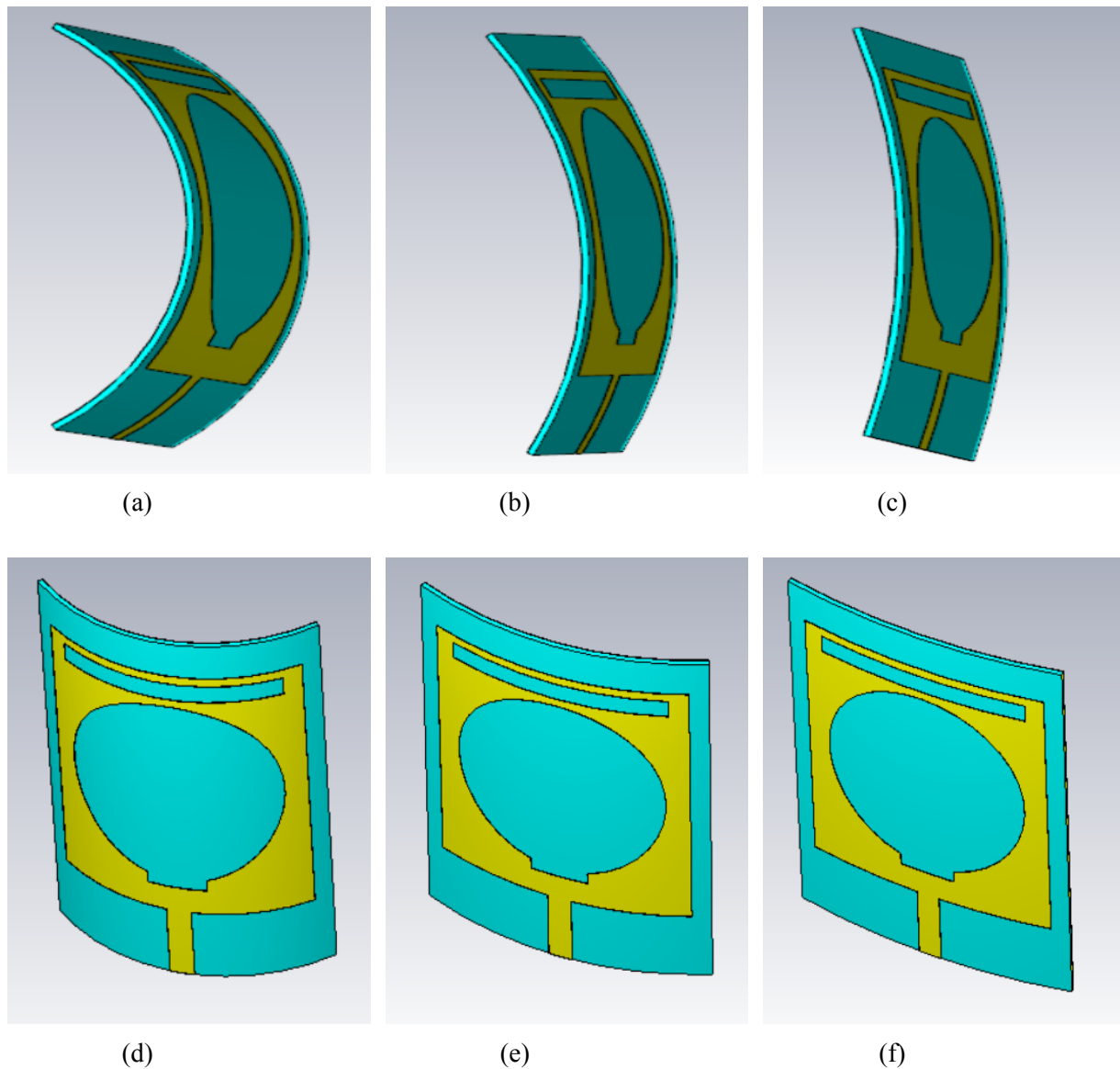


Figure 5.26: Structure of antenna under two bending condition with different radii, horizontal (x-axis) (a) $R_x = 20$ mm, (b) $R_x = 40$ mm, (c) $R_x = 80$ mm and Vertical (y-axis) (d) $R_y = 20$ mm, (e) $R_y = 40$ mm, (f) $R_y = 80$ mm

The results of the simulations in each scenario of bending indicated that there is little to no change in the resonance frequency and S11 characteristic of the antennas. Additionally, the bending of the antenna is seen to boost gain. Table 5.3 contains a summary of the findings of the bending analysis.

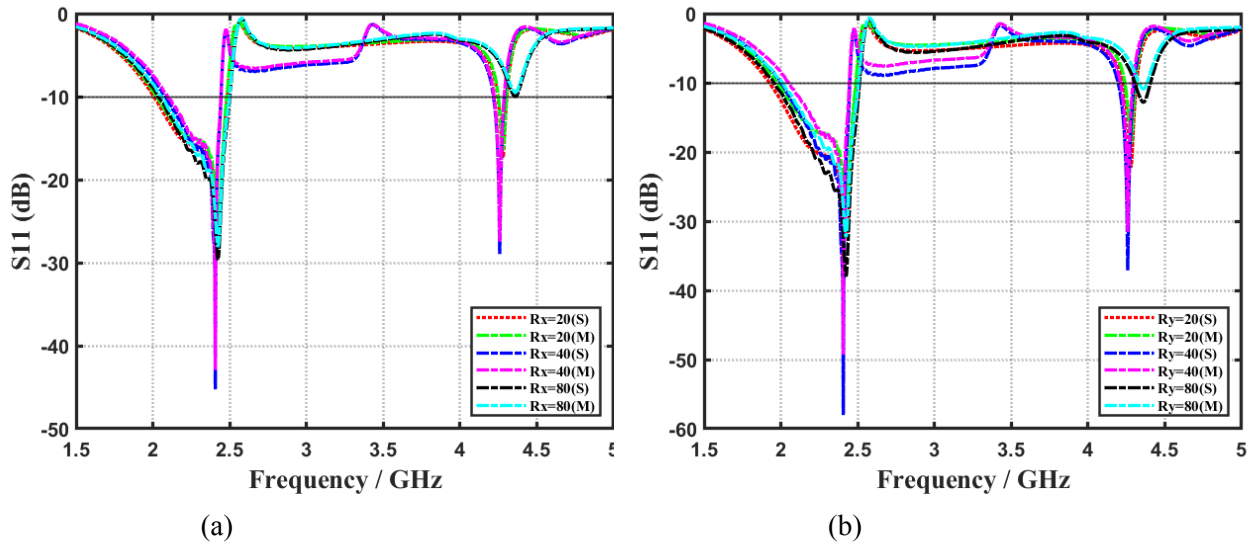


Figure 5.27: Measured and simulated S11(s) of the proposed antenna under (a) horizontal (x-axis) and (b) vertical (y-axis) bending conditions with different curvatures

The purposed antenna is flexible, making it suitable for usage in bending settings, according to the results, which were acquired.

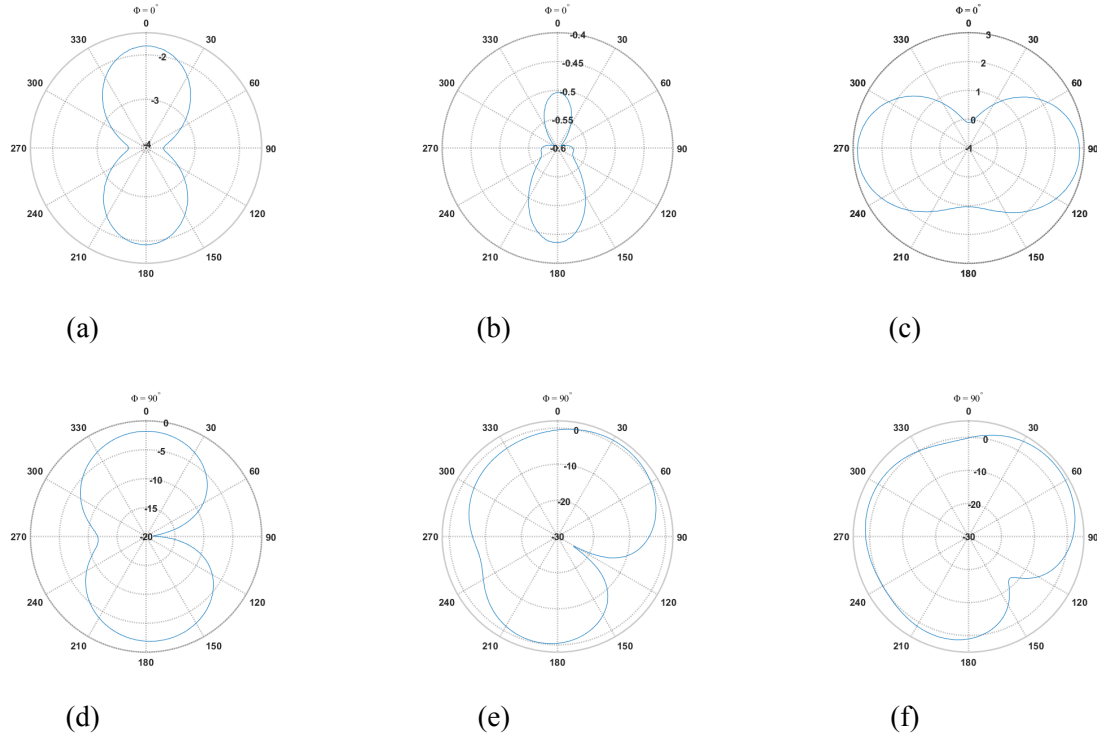


Figure 5.28: Radiation pattern of antenna under horizontal (x-axis) bending condition with different radii, E-plane ($\phi = 0^\circ$) and (b)(a) Rx = 20 mm, (b) Rx = 40 mm, (c) Rx = 80 mm and H-plane ($\phi = 90^\circ$)(d) Rx = 20 mm, (e) Rx = 40 mm, (f) Rx = 80 mm

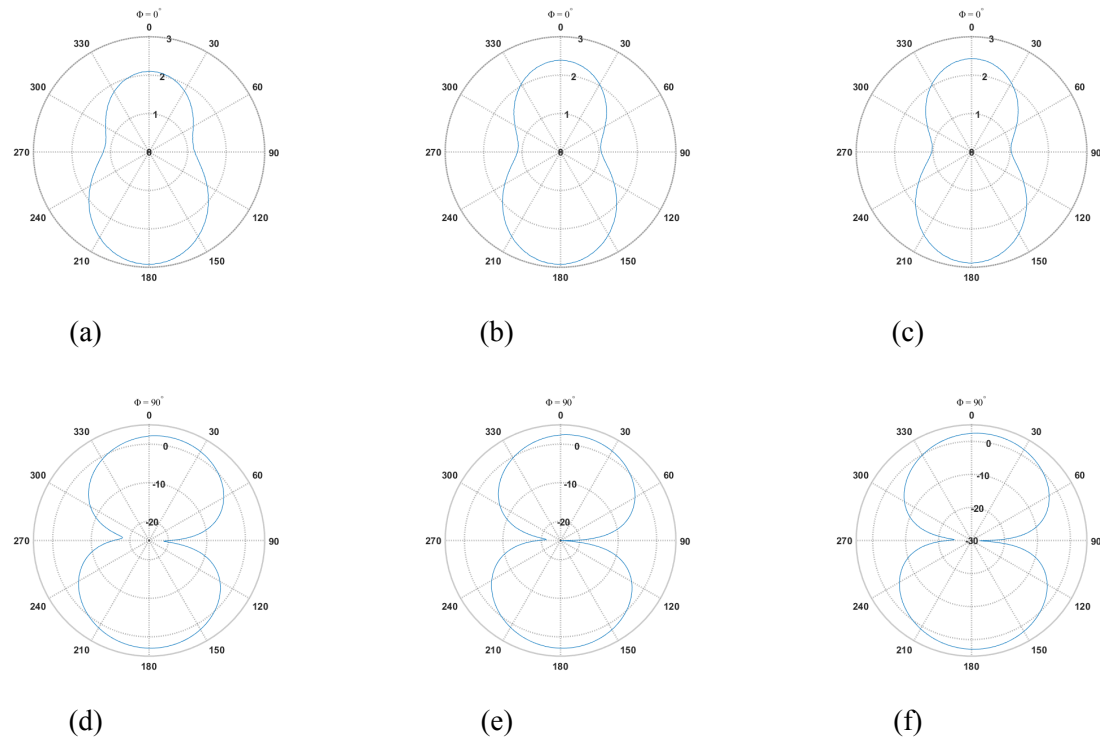


Figure 5.29: Radiation pattern of antenna under vertical (y-axis) bending condition with different radii, E-plane ($\phi = 0^\circ$) and (b)(a) $R_x = 20$ mm, (b) $R_x = 40$ mm, (c) $R_x = 80$ mm and H-plane ($\phi = 90^\circ$)(d) $R_x = 20$ mm, (e) $R_x = 40$ mm, (f) $R_x = 80$ mm

Table 5.3

Comparison of antenna properties under two bending conditions with different curvatures

Bending in x-axis (Horizontal)				Bending in y-axis (Vertical)			
R_x (mm)	Res. freq (GHz)	S11 (dB)	Gain (dBi)	R_y (mm)	Res. freq (GHz)	S11 (dB)	Gain (dBi)
Unbent	2.45	-41.72	2.62	Unbent	2.45	-41.72	2.62
20	2.431	-25.38	2.87	20	2.43	-32.54	2.93
40	2.40	-45.25	2.73	40	2.40	-58.01	2.94
80	2.42	-29.63	2.68	80	2.42	-37.98	2.92

5.1.4 Comparision of the proposed antennas with previous work

To assess the effectiveness of the proposed antennas, a comparative analysis was carried out with existing wearable antennas, as detailed in Table 5.3. The evaluation parameters included size, substrate material and Bandwidth. Based on the analysis, the proposed antenna was found to be relatively

compact, exhibited satisfactory radiation performance, and complied with the prescribed SAR limits.

Table 5.4
Comparision of proposed antennas with other wearable antennas

Ref.	Dimensions (mm³)	Frequency (GHZ)	S11 (dB)	Gain (dBi)	Substrate
[13]	70 x 50 x 0.66	1.198-4.055	-26	2.9	Polyester fibre
[14]	55.8 x 47.4 x 2	2-3	<-20	3.2	Cotton fabric
[15]	85.5 x 85.5 x 5.62	1.4-2.4	-16	1.94	Kelver
[16]	55 x 40 x 0.125	1.77-6.95	<-30	2.6	Kapton polymide
[19]	39 x 39 x 0.508	2.36-2.55	<-30	2.06	RogersRT
[26]	70 x 70 x 2.26	2.36-2.40	-30	1.38	Wolf felt
[27]	59.8 x 59.8 x 3.18	2.3-2.68	-20	2.64	PDMS
[28]	38.1 x 38.1 x 2	2.4-2.485	-35	2.79	Felt
[29]	40 x 40 x 1.6	1.71-3.94	-30.1	1.96-2.36	FR4
[30]	72.54 x 72.54 x 1.67	2.4-2.5	-18, -23	1.92, 2.27	Felt&jeans, Felt&telfon
Design 1	44 x 45.2 x 0.6	1.895 - 2.909	- 29.225	1.828	Jeans
Design 2	36 x 55 x 0.6	1.68-2.48	-41	3.6	Jeans
Design 3	31 x 42 x 0.6	2.19 - 2.57	- 41.72	2.62	Jeans

Chapter 6

CONCLUSION

This chapter provides a concluding summary of the entire project.

6.1 Conclusion

We have developed highly flexible fabric antennas that are compact and low-profile, making them ideal for use in Wireless Body Area Networks. By incorporating rectangular, circular slots, and Koch fractal design in the conventional rectangular patch, we were able to achieve miniaturization and impedance matching of the antennas. To further improve the gain of the antennas, we utilized a DGS ground plane. All the proposed antennas resonate at 2.45 GHz with an exceptional reflection coefficient, gain, and radiation efficiency. Notably, the proposed antenna designs demonstrate exceptional performance when subjected to bending along both the x and y axes. Additionally, these antennas comply with the strict SAR guidelines outlined by both the IEEE and FCC regulatory bodies. Overall, the proposed designs exhibit superior performance and represent a highly promising solution for use in human wearable devices. Based on the bandwidth, radiation efficiency, and gain requirements, Any one of these designs can be chosen accordingly.

REFERENCES

- [1] A. Smida, A. Iqbal, A. J. Alazemi, M. I. Waly, R. Ghayoula and S. Kim, "Wideband Wearable Antenna for Biomedical Telemetry Applications," in IEEE Access, vol. 8, pp. 15687-15694, 2020.
- [2] Y. J. Li, Z. Y. Lu and L. S. Yang, "CPW-Fed Slot Antenna for Medical Wearable Applications," in IEEE Access, vol. 7, pp. 42107-42112, 2019.
- [3] M. M. H. Mahfuz et al., "Wearable Textile Patch Antenna: Challenges and Future Directions," in IEEE Access, vol. 10, pp. 38406-38427, 2022.
- [4] U. Ali, S. Ullah, B. Kamal, L. Matekovits and A. Altaf, "Design, Analysis and Applications of Wearable Antennas: A Review," in IEEE Access, vol. 11, pp. 14458-14486, 2023.
- [5] K. N. Paracha, S. K. Abdul Rahim, P. J. Soh and M. Khalily, "Wearable Antennas: A Review of Materials, Structures, and Innovative Features for Autonomous Communication and Sensing," in IEEE Access, vol. 7, pp. 56694-56712, 2019.
- [6] Puttaswamy, Prasanna & Srivatsa, Pramod & Murthy, Krishna & Thomas, Bindu. (2014). Analysis of loss tangent effect on Microstrip antenna gain. International Journal of Applied Science and Engineering Research. 3. 10.6088/ijaser.030600011.
- [7] Priya, Ankita & Kumar, Ayush & Chauhan, Brajlata. (2015). A Review of Textile and Cloth Fabric Wearable Antennas. International Journal of Computer Applications. 116. 975-8887. 10.5120/20425-2741.
- [8] Ibanez-Labiano I, Alomainy A. Dielectric Characterization of Non-Conductive Fabrics for Temperature Sensing through Resonating Antenna Structures. Materials (Basel). 2020 Mar 11;13(6):1271.
- [9] J. Singh, A. Kaur, J. Kaur and E. Sidhu, "High gain textile microstrip patch antenna design employing denim substrate for Ku band satellite applications," 2016 International Conference on Control, Computing, Communication and Materials (ICCCCM), Allahbad, India, 2016, pp. 1-5.
- [10] M. Kowsalya, T. R. Muthu and S. Murugan, "Design and implementation of flexible microstrip antenna for ISM band applications," 2017 International Conference on Innovations in Information, Embedded and Communication Systems (ICIIECS), Coimbatore, India, 2017, pp. 1-4.
- [11] Turkmen, M., & Yalduz, H. (2018). Design and Performance Analysis of a Flexible UWB Wearable Textile Antenna on Jeans Substrate. International Journal of Information and Electronics Engineering, 8(2), 15-18.
- [12] M. M. Ur Rashid, A. Rahman, L. C. Paul and A. Krishno Sarkar, "Performance Evaluation of a Wearable 2.45 GHz Planar Printed Meandering Monopole Textile Antenna on Flexible Substrates,"

REFERENCES

- 2019 1st International Conference on Advances in Science, Engineering and Robotics Technology (ICASERT), Dhaka, Bangladesh, 2019, pp. 1-6.
- [13] X. Lin, Y. Chen, Z. Gong, B. -C. Seet, L. Huang and Y. Lu, "Ultrawideband Textile Antenna for Wearable Microwave Medical Imaging Applications," in IEEE Transactions on Antennas and Propagation, vol. 68, no. 6, pp. 4238-4249, June 2020.
- [14] S. Alharbi and A. Kiourtzi, "Folding-Dependent vs. Folding-Independent Flexible Antennas on E-Textiles," 2019 IEEE International Symposium on Antennas and Propagation and USNC-URSI Radio Science Meeting, Atlanta, GA, USA, 2019, pp. 755-756.
- [15] R. Joshi et al., "Dual-Band, Dual-Sense Textile Antenna With AMC Backing for Localization Using GPS and WBAN/WLAN," in IEEE Access, vol. 8, pp. 89468-89478, 2020.
- [16] H. F. Abutarboush, W. Li and A. Shamim, "Flexible-Screen-Printed Antenna With Enhanced Bandwidth by Employing Defected Ground Structure," in IEEE Antennas and Wireless Propagation Letters, vol. 19, no. 10, pp. 1803-1807, Oct. 2020.
- [17] Abdullah G. Al-Sehemi, Ahmed A. Al-Ghamdi, Nikolay T. Dishovsky, Nikolay T. Atanasov & Gabriela L. Atanasova (2017) Flexible and small wearable antenna for wireless body area network applications, Journal of Electromagnetic Waves and Applications, 31:11-12, 1063-1082.
- [18] S. Das and D. Mitra, "A Compact Wideband Flexible Implantable Slot Antenna Design With Enhanced Gain," in IEEE Transactions on Antennas and Propagation, vol. 66, no. 8, pp. 4309-4314, Aug. 2018.
- [19] A. Arif, M. Zubair, M. Ali, M. U. Khan and M. Q. Mehmood, "A Compact, Low-Profile Fractal Antenna for Wearable On-Body WBAN Applications," in IEEE Antennas and Wireless Propagation Letters, vol. 18, no. 5, pp. 981-985, May 2019.
- [20] I. Gil & R. Fernández-García (2017) Wearable PIFA antenna implemented on jean substrate for wireless body area network, Journal of Electromagnetic Waves and Applications, 31:11-12, 1194-1204.
- [21] Noor, Shehab & Ramli, Nurulazlina & Hanapi, Nurul. (2020). A Review of the Wearable Textile-Based Antenna using Different Textile Materials for Wireless Applications. Open Journal of Science and Technology. 3. 10.31580/ojst.v3i3.1665.
- [22] C. A. Balanis, Antenna theory: analysis and design. John wiley & sons, 2015.
- [23] A. Y. I. Ashyap et al., "Robust and Efficient Integrated Antenna With EBG-DGS Enabled Wide Bandwidth for Wearable Medical Device Applications," in IEEE Access, vol. 8, pp. 56346-56358, 2020.

REFERENCES

- [24] M. Wang et al., "Investigation of SAR Reduction Using Flexible Antenna With Metamaterial Structure in Wireless Body Area Network," in IEEE Transactions on Antennas and Propagation, vol. 66, no. 6, pp. 3076-3086, June 2018.
- [25] "IEEE Standard for Safety Levels with Respect to Human Exposure to Electric, Magnetic, and Electromagnetic Fields, 0 Hz to 300 GHz," in IEEE Std C95.1-2019 (Revision of IEEE Std C95.1-2005/ Incorporates IEEE Std C95.1-2019/Cor 1-2019) , vol., no., pp.1-312, 4 Oct. 2019.
- [26] H. Yang and X. Liu, "Wearable Dual-Band and Dual-Polarized Textile Antenna for On- and Off-Body Communications," in IEEE Antennas and Wireless Propagation Letters, vol. 19, no. 12, pp. 2324-2328, Dec. 2020.
- [27] R. B. V. B. Simorangkir, Y. Yang, K. P. Esselle and B. A. Zeb, "A Method to Realize Robust Flexible Electronically Tunable Antennas Using Polymer-Embedded Conductive Fabric," in IEEE Transactions on Antennas and Propagation, vol. 66, no. 1, pp. 50-58, Jan. 2018.
- [28] H. Li, S. Sun, B. Wang and F. Wu, "Design of Compact Single-Layer Textile MIMO Antenna for Wearable Applications," in IEEE Transactions on Antennas and Propagation, vol. 66, no. 6, pp. 3136-3141, June 2018.
- [29] A. Iqbal, A. Smida, A. J. Alazemi, M. I. Waly, N. Khaddaj Mallat and S. Kim, "Wideband Circularly Polarized MIMO Antenna for High Data Wearable Biotelemetric Devices," in IEEE Access, vol. 8, pp. 17935-17944, 2020.
- [30] Mustafa, A.B., Rajendran, T. An Effective Design of Wearable Antenna with Double Flexible Substrates and Defected Ground Structure for Healthcare Monitoring System. *J Med Syst* 43, 186 (2019).
- [31] S. Alharbi, R. M. Shubair and A. Kiourtzi, "Flexible antennas for wearable applications: Recent advances and design challenges," 12th European Conference on Antennas and Propagation (EuCAP 2018), London, UK, 2018, pp. 1-3.
- [32] A. Nathan et al., "Flexible Electronics: The Next Ubiquitous Platform," in Proceedings of the IEEE, vol. 100, no. Special Centennial Issue, pp. 1486-1517, 13 May 2012.
- [33] Jhunjhunwala, Vikash Kumar, Tanweer Ali, Pramod Kumar, Praveen Kumar, Pradeep Kumar, Sakshi Shrivastava, and Arnav Abhijit Bhagwat. 2022. "Flexible UWB and MIMO Antennas for Wireless Body Area Network: A Review" *Sensors* 22, no. 23: 9549.
- [34] E. M. Shareena, P. Abdulla and B. Lethakumary, "Analysis of transmitting wire antenna," 2012 International Conference on Power, Signals, Controls and Computation, Thrissur, India, 2012, pp. 1-7.

REFERENCES

- [35] J. C. Wang, M. Leach, Z. Wang, E. G. Lim, K. L. Man and Y. Huang, "Wireless body area network and its applications," 2015 International SoC Design Conference (ISOCC), Gyeongju, Korea (South), 2015, pp. 169-170.
- [36] D. Le, S. Ahmed, L. Ukkonen and T. Björnin, "A Small All-Corners-Truncated Circularly Polarized Microstrip Patch Antenna on Textile Substrate for Wearable Passive UHF RFID Tags," in IEEE Journal of Radio Frequency Identification, vol. 5, no. 2, pp. 106-112, June 2021.
- [37] U. R. Khan, J. A. Sheikh, A. Junaid, R. Amin, S. Ashraf and S. Ahmed, "Design of a Compact Hybrid Moore's Fractal Inspired Wearable Antenna for IoT Enabled Bio-Telemetry in Diagnostic Health Monitoring System," in IEEE Access, vol. 10, pp. 116129-116140, 2022.
- [38] S. Ahmed, S. T. Qureshi, L. Sydänheimo, L. Ukkonen and T. Björnin, "Comparison of Wearable E-Textile Split Ring Resonator and Slotted Patch RFID Reader Antennas Embedded in Work Gloves," in IEEE Journal of Radio Frequency Identification, vol. 3, no. 4, pp. 259-264, Dec. 2019.

LIST OF PUBLICATIONS

1. Antenna Design 2 have been submitted for SCI Wireless Networks Journal.
2. Antenna Design 3 have been submitted for SCI Wireless Personal Communications Journal.



